DATA DRIVEN ANALYSIS SAMARA SEED KINEMATICS AND DYNAMICS

Shashwat Sparsh

Advisor: Dr. Nandeesh Hiremath

BACKGROUND

BACKGROUND

Samara Seed: class of fruit most famous from the *Acer* genus (Maples)

Colloquially known as “helicopter” plants

Exhibit auto-rotating behavior as they fall

Walter Siegmund, CC BY-SA 3.0 <https://creativecommons.org/licenses/by-sa/3.0>, via Wikimedia Commons

STAGES OF FLIGHT

- Free Fall: Kinematics modeled by Free Fall
- Transition:
  - Time period between the end of free-fall and the start of steady-state rotation like a helicopter
  - Not the subject of most aerodynamic studies
- Steady-State:
  - Seed exhibits auto-rotation and lower descent velocity
  - Primary focus of most studies
- Initial attitude and form factor have a significant impact
- Small Aerodynamic Torque in the initial drop perturbed the to generate rotation

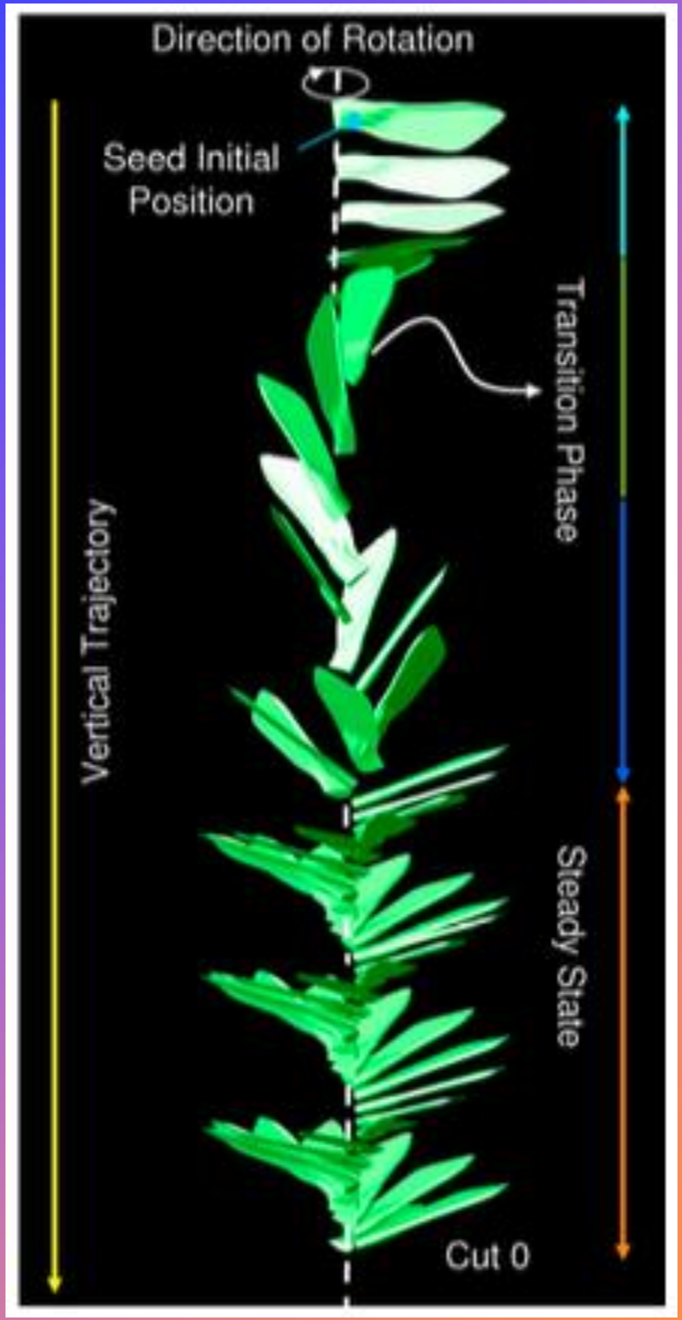

[Reference 14]

PREVIOUS RESEARCH

- Biological Studies
  - “Efficient Seed Dispersal”
  - Morphological Property Distribution
- Aerodynamic Studies
  - Particle Image Velocimetry (PIV) Flow Analysis: Strong Leading-Edge Vortex (LEV) formation
  - Geometric and Flight Characteristic relations
  - Simulation Models
- Aerodynamic analysis does not necessarily agree with Biological studies

MOTIVATIONAL QUESTIONS

- Do the single-bladed seeds undergoing auto-rotation truly support the widely accepted claim of seed dispersal?
- Is there any peculiar morphological or flight characteristics that make a minority number of seeds fly far distances?
- What relationships are present between the flight performance and geometric characteristics?
- Investigate the kinematic and dynamic responses during steady-state and transition
- Applications:
  - Biomimicry
  - Large Scale Terraforming via seed dispersal

BIOLOGICAL STUDIES

WIND DRIFT

- Literature Review: Wind Drift studies are predominantly biological and statistical regarding dispersion
- Performance:
  - Greater than seeds that fall straight down
  - Poorer than fruit using *tufted* methods

PIV STUDIES

MODELING WAKE FLOW

Identification of appropriate Wake State

Local flow over the samara blade characterized by a Leading Edge Vortex (LEV)

Wing-root vortex, root-tip vortex, and wing-tip vortex in wake

Multiple tests of single samara specifically during steady-state auto-rotation

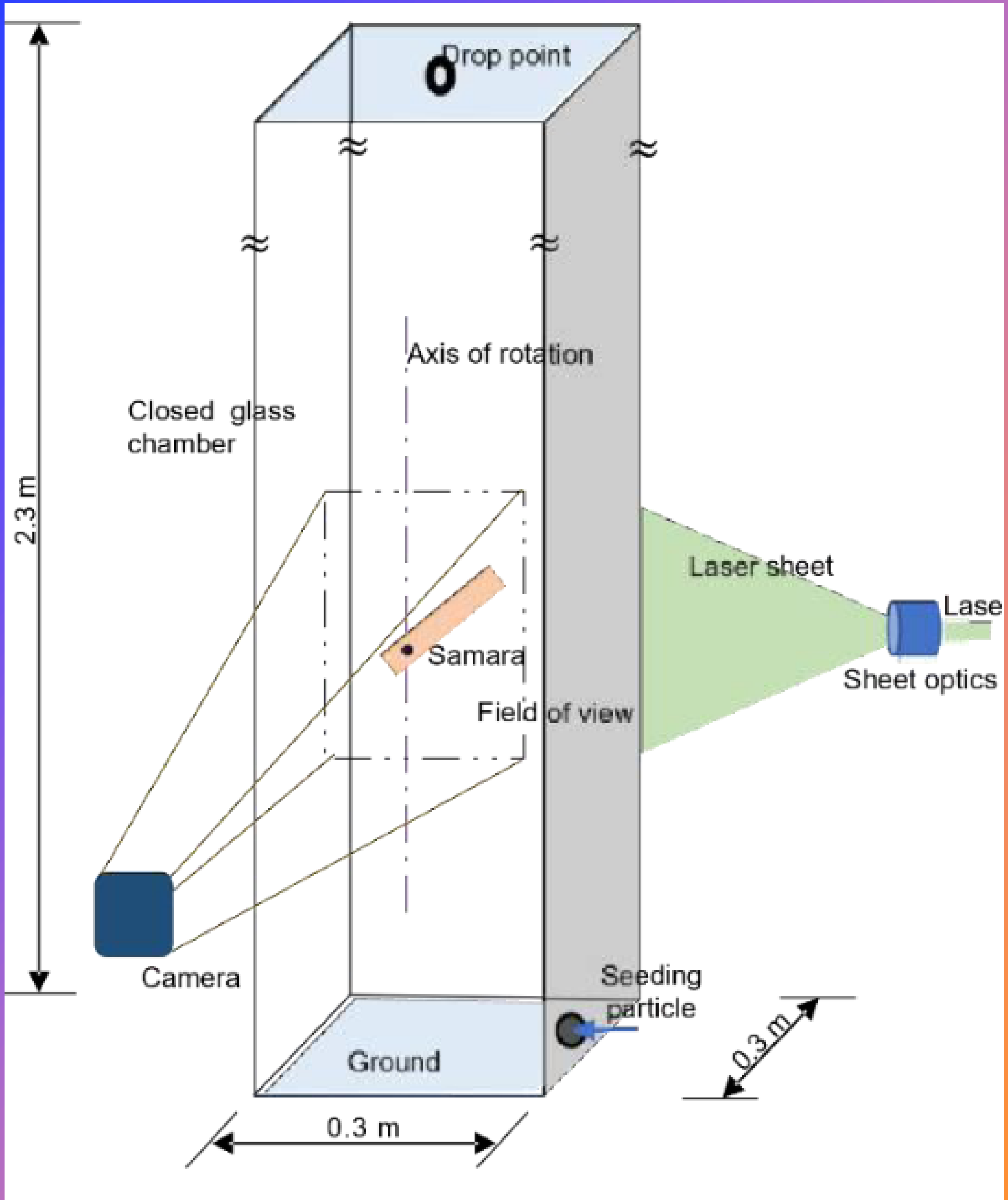

NORMAL WORKING STATE: VERTICAL CLIMB

- Continuous Contraction of slipstream above, through, and below rotor
- Upstream: Above Rotor
- Downstream: Below Rotor
- Induced Velocity: γ
- Rotor Climb Velocity: V_H
- Down Stream Velocity: V_D

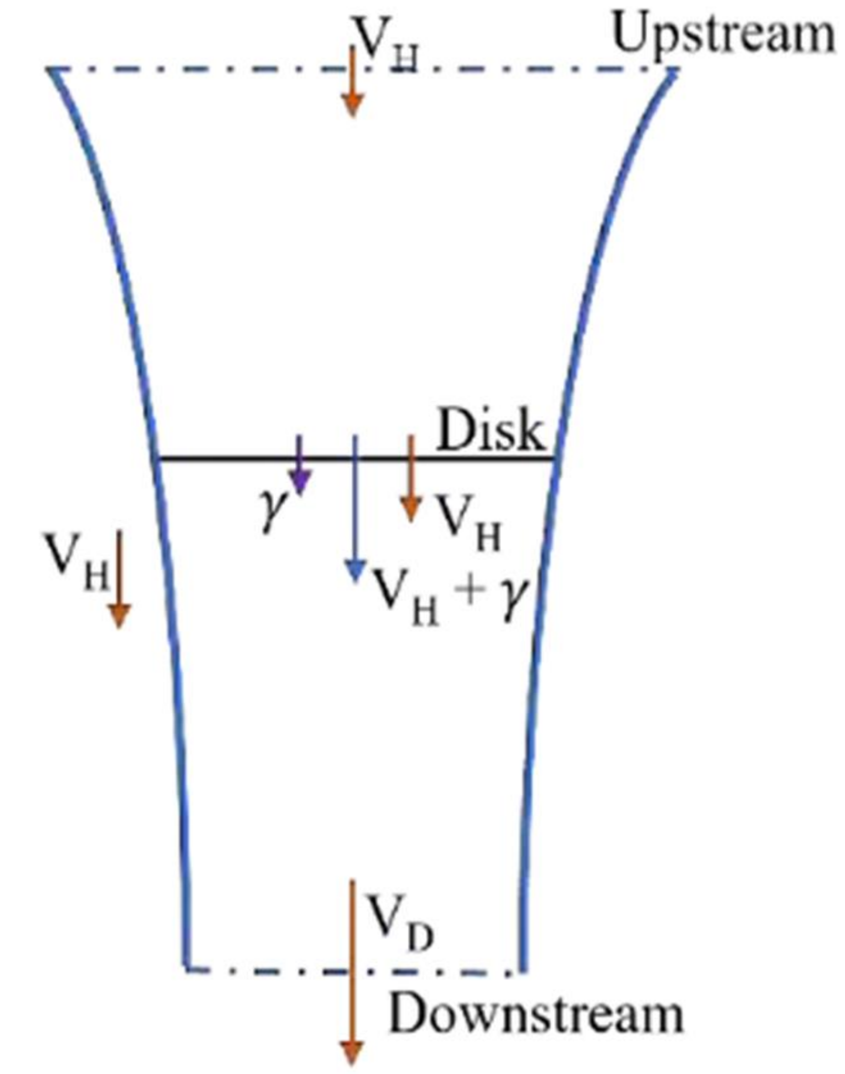

A. Hovering or vertical climb

VORTEX-RING STATE: DESCENT

- External flow is upward
- Net flow is downward
- Flow is Steady
- Upstream: Below Rotor
- Downstream: Above Rotor
- $\gamma \gg V$
- Rotor Descent Velocity : V
- Down Stream Velocity: V_D

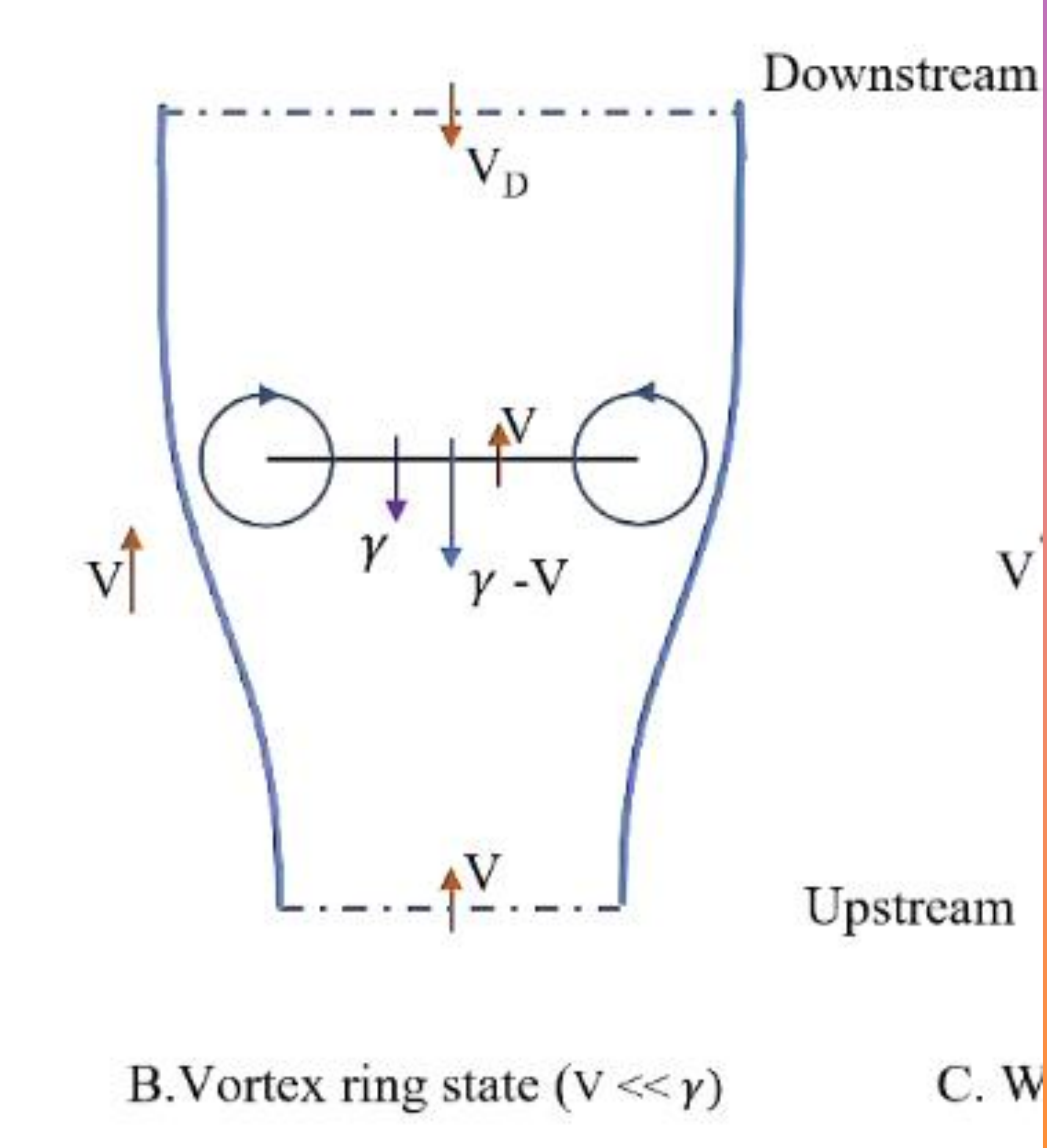

WINDMILL BRAKE STATE: DESCENT

- $\boldsymbol{\gamma \ll V}$
- $V_{Vortex} < V_{Windmill}$
- Definite Slipstream Expanding as it passes upward
- Upstream: Below Rotor
- Downstream: Above Rotor
- Windmill extracting energy from the wind

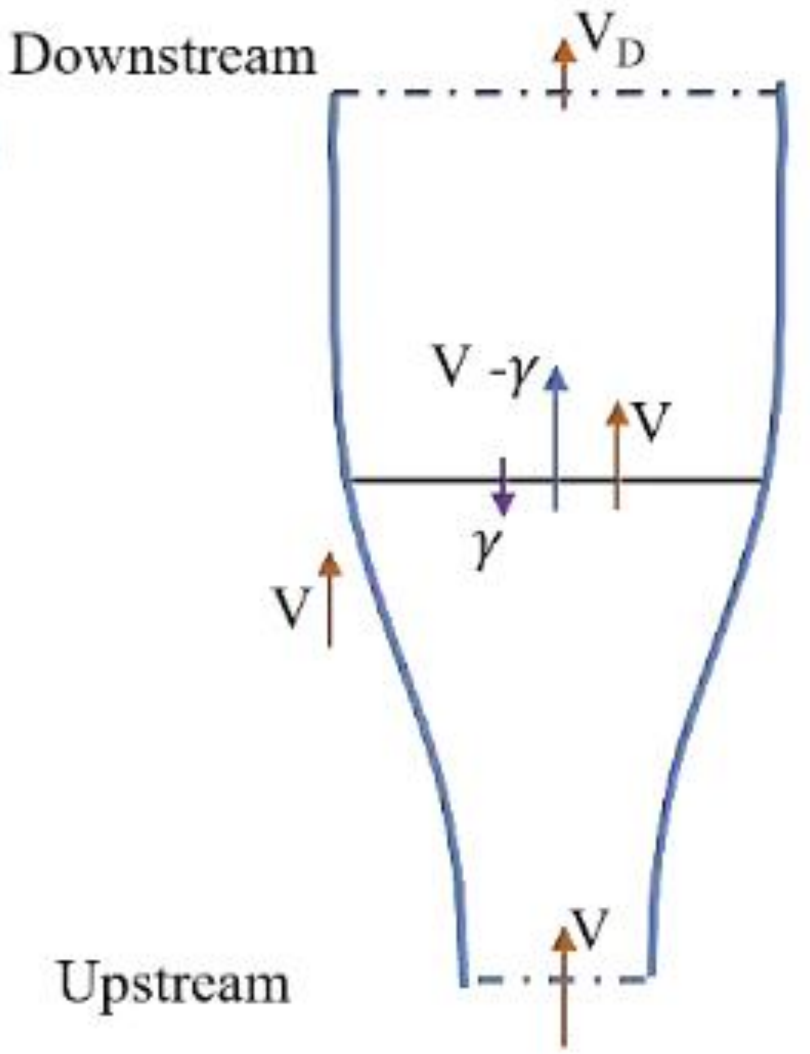

C. Windmill brake state ($V >> \gamma$)

MODELING WAKE FLOW

4 Distinct Regions: Wake core flow, Upstream regions, Vortices region, and outer-wake

Vertical and Horizontal offsets between vortices

Coning Angle of 24° poor flat disk approximation

Wingtip Velocity combines the induced and descent velocity terms

Wake Flow characterized as the **windmill brake model**: $v_y > 0$ throughout the field

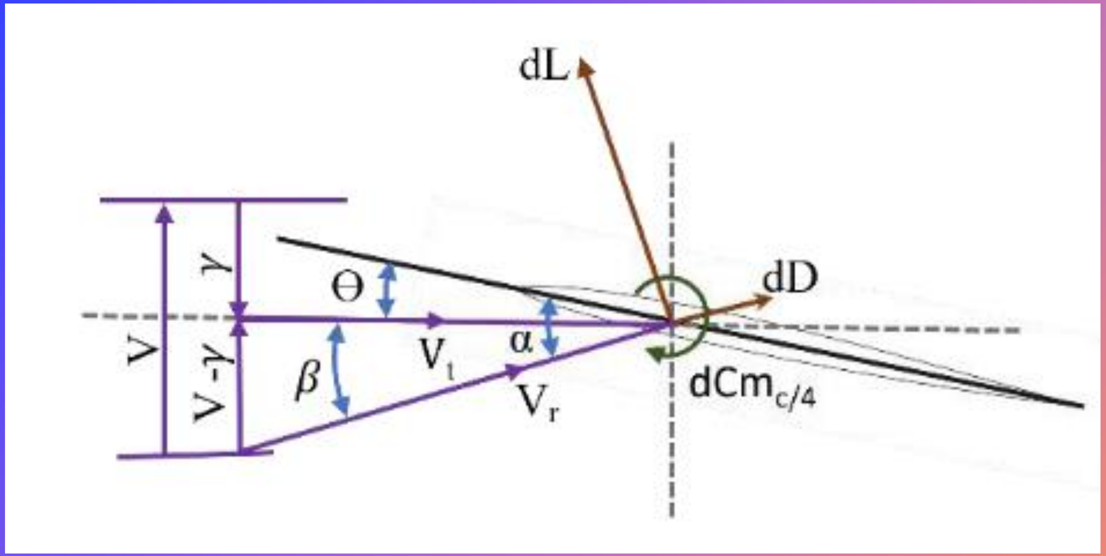

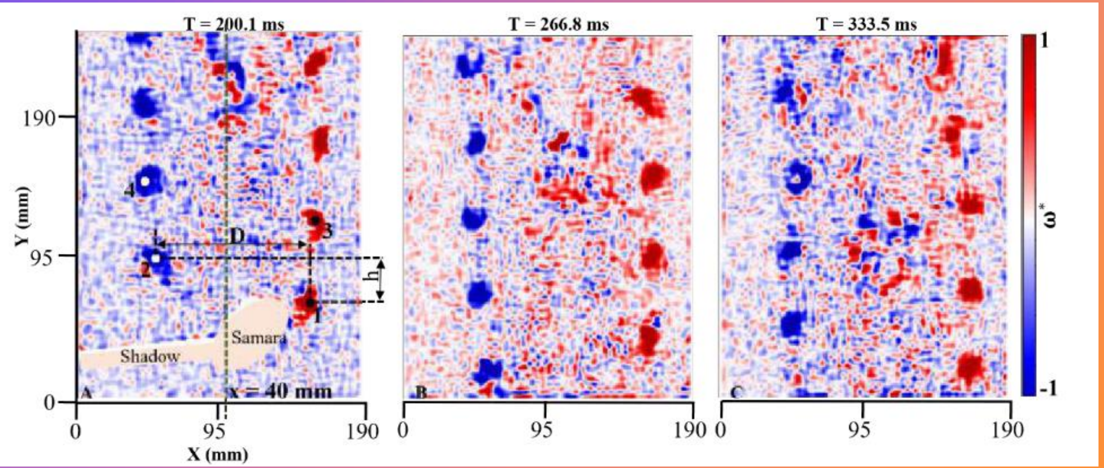

MECHANISM OF AUTOROTATION

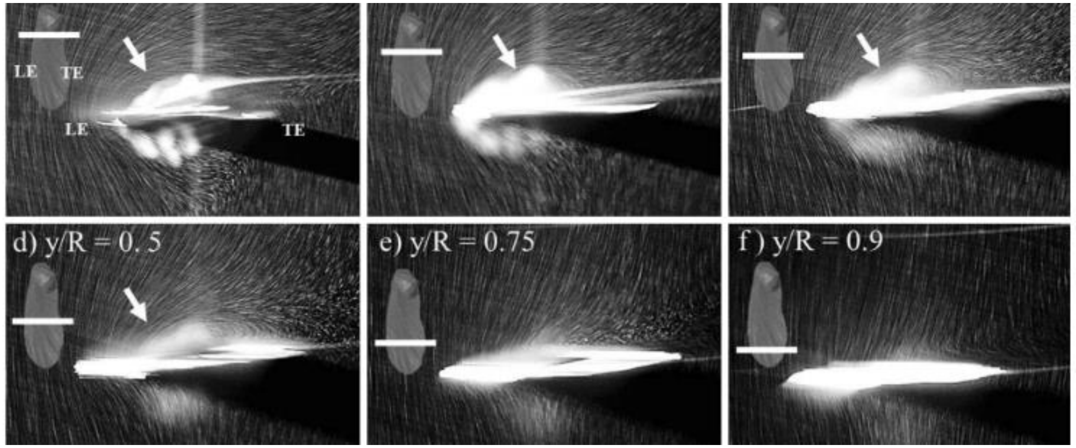

- Autorotation: Equilibrium velocity established by force balance of aerodynamic and gravitational forces
- Seeds were dropped in a vertical wind tunnel and made to hover with coning angle $\beta = 0°$ and pitch angle $\theta = 1.5°$
- Compact LEVS:
  - Form even at high angles of attack $\alpha \approx 60°$
  - **Begin at 25% span and dissipate at 90% span**
- Results are specific to Swietenia genus

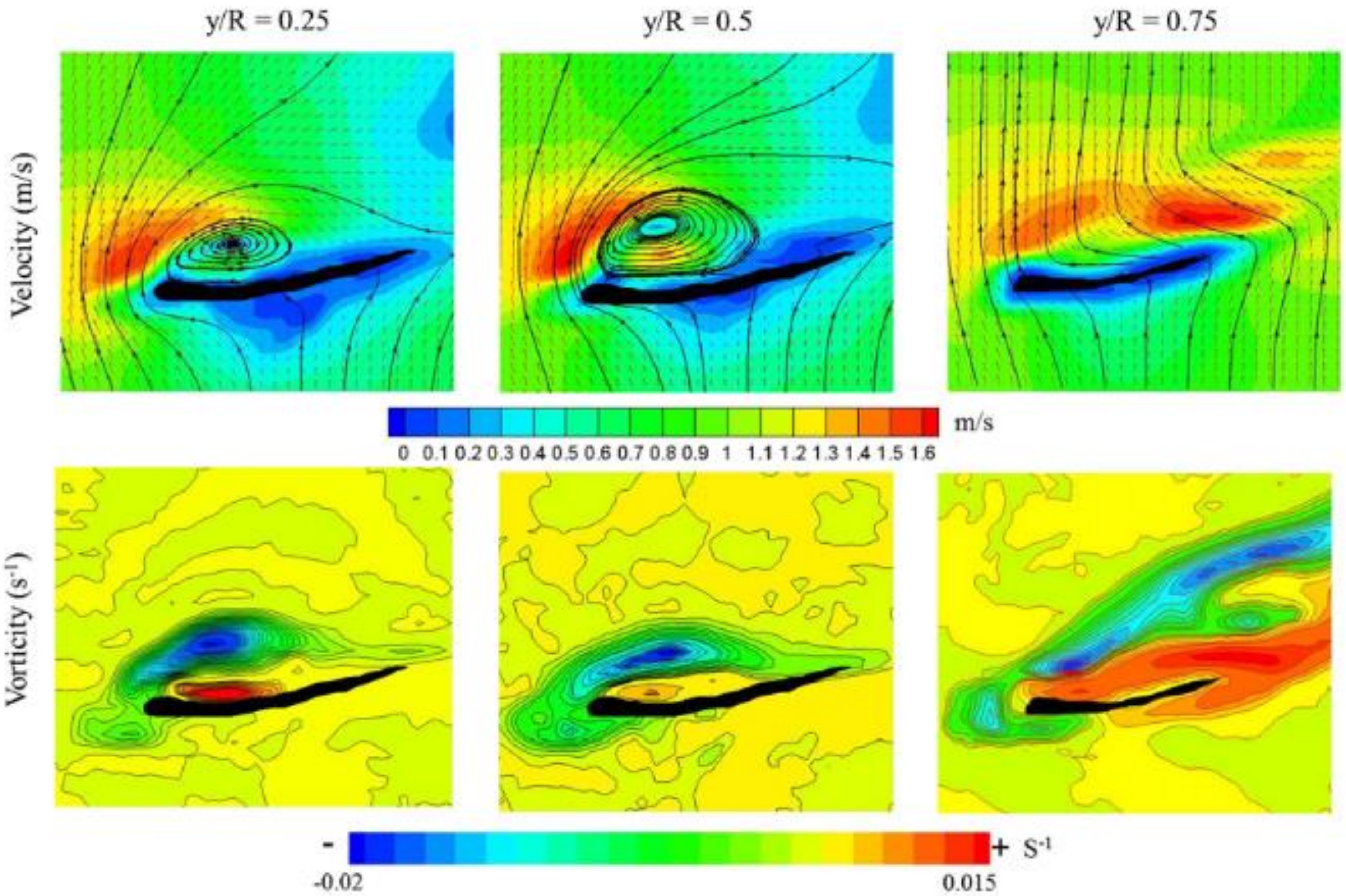

y/R = 0.25
y/R = 0.5
y/R = 0.75
Velocity (m/s)
m/s
0 0.1 0.2 0.3 0.4 0.5 0.6 0.7 0.8 0.9 1 1.1 1.2 1.3 1.4 1.5 1.6
Vorticity (s-1)
- + S-1
-0.02
0.015

Morphological Impact on Aerodynamics

GEOMETRIC PROPERTY STUDIES

GEOMETRIC IMPACT: MORPHOLOGICAL PERTURBATION

Multi-Species Test

Hover test in vertical wind tunnel

Descent Velocity Prediction Models

- Standard Model: $mg/A \sim V_D^2$
- Proposed Model: $mg \sim .5C_D\rho V_D^2 A\cos\theta$

Descent velocity has little to no apparent correlation with coning angle (θ) or angular velocity (ω)

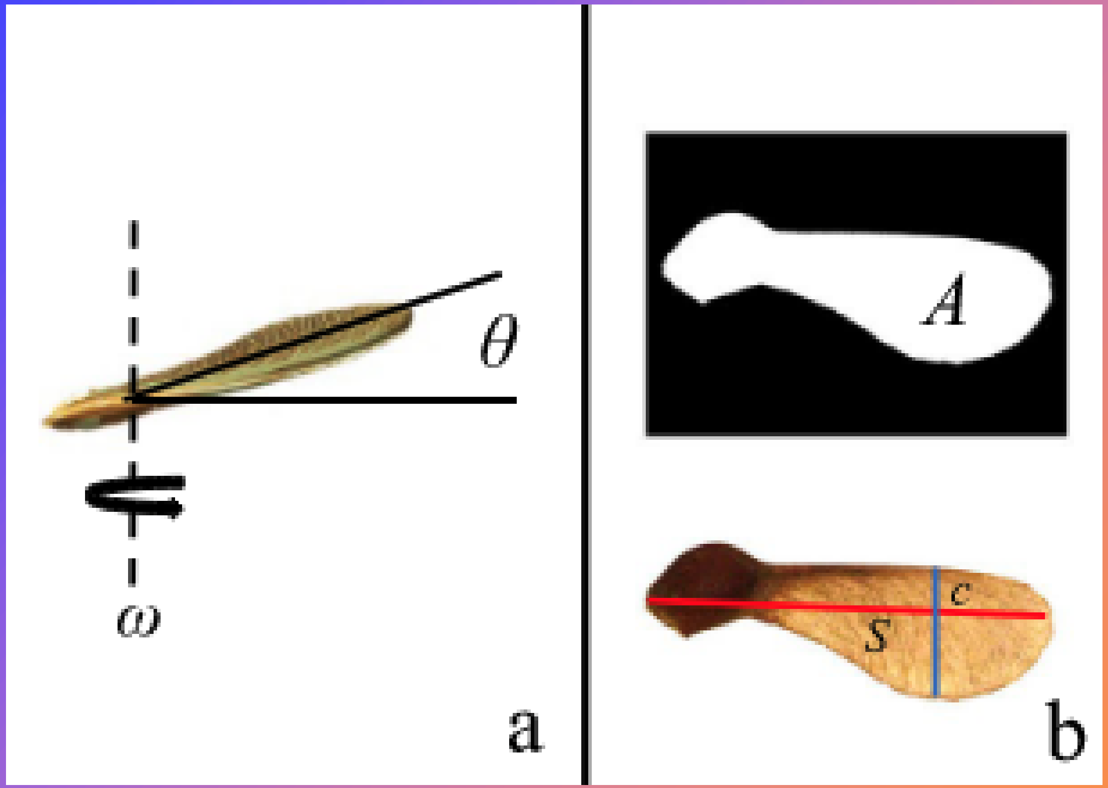

MORPHOLOGICAL PERTURBATION

±70% mass changes correspond to ±15% changes in descent velocity

Chord is the most appropriate parameter for characterizing seeds

Significant variance in masses across samples

Performance is more complicated than $mg/A \sim V_D^2$

Better Performance Predictor:
$\boldsymbol{mg \sim .5 C_D \rho V_D^2 A \cos\theta}$

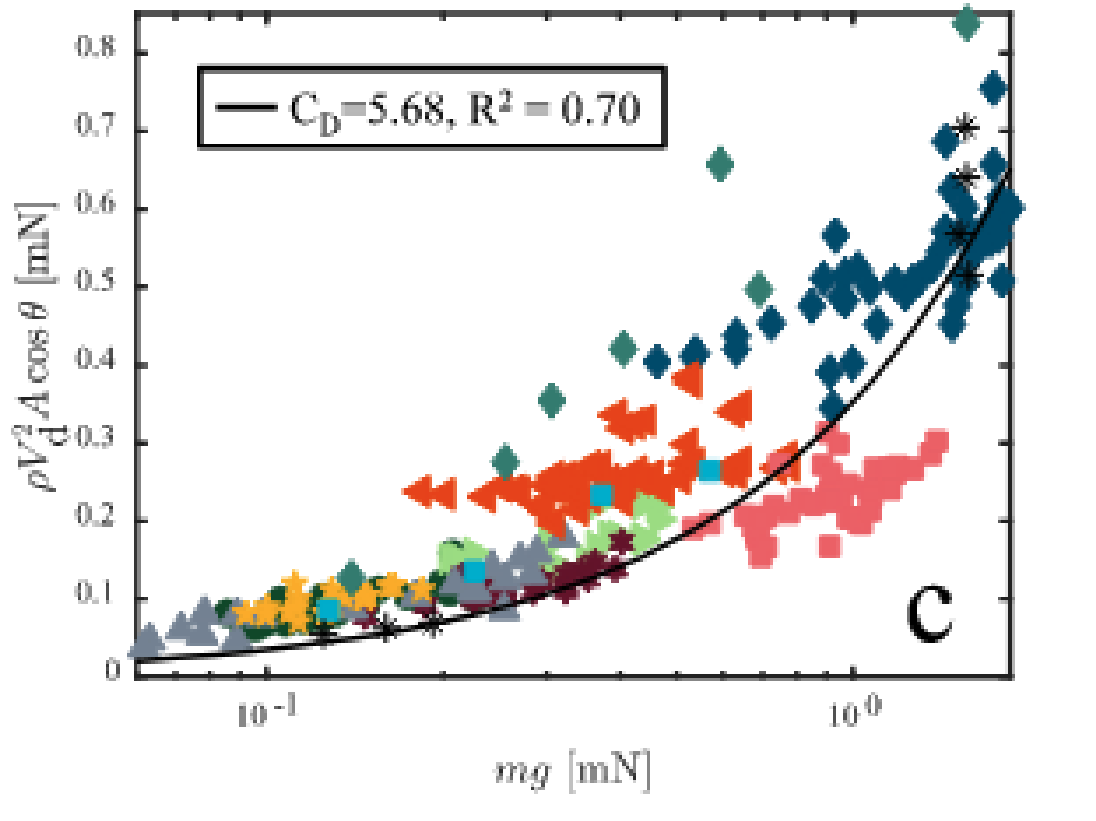

GEOMETRIC IMPACT: ROTATIONAL EFFICIENCY

Mechanical samara models

- Planar symmetric blade
- Low Reynolds number flight regime

Consistent transition to steady-state rotation with drastically different trajectories

Fourier Series Model

- **Successful extraction of Roll, Pitch, and Yaw rates**
- Increasing phase between roll and pitch rates corresponds to increasing radius of precession

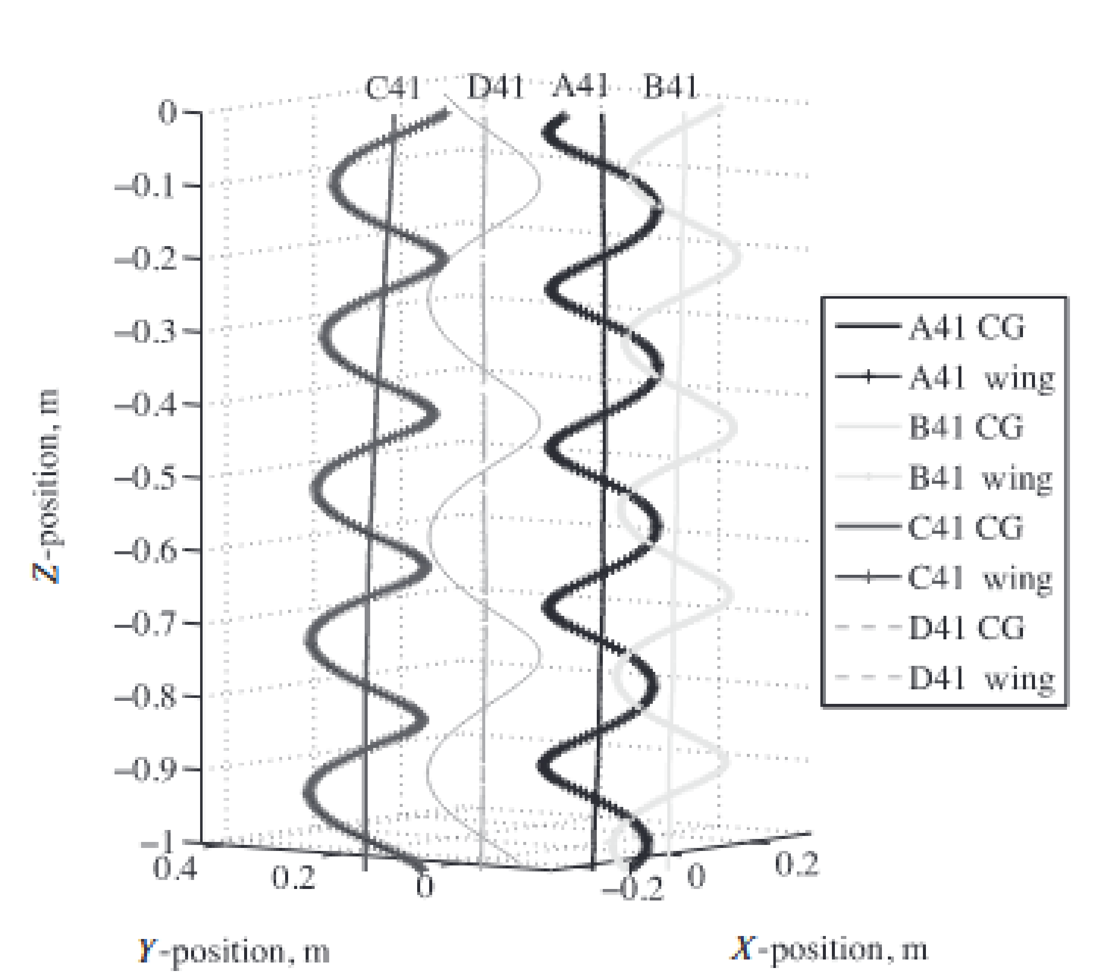

Table 2. Physical properties of the mechanical samaras

Physical Property	Units	A41	B41	C41	D41
I_{11}	kg m^2	9.64×10^{-6}	7.62×10^{-6}	1.00×10^{-5}	7.65×10^{-6}
I_{22}	kg m^2	4.99×10^{-7}	5.80×10^{-7}	5.16×10^{-7}	6.59×10^{-7}
I_{33}	kg m^2	1.01×10^{-5}	8.18×10^{-6}	1.05×10^{-5}	8.29×10^{-6}
Span of wing	m	0.168	0.150	0.168	0.135
Mass	kg	0.00526	0.00526	0.00526	0.00526
Surface area	m^2	1.24×10^{-2}	1.24×10^{-2}	1.24×10^{-2}	1.24×10^{-2}

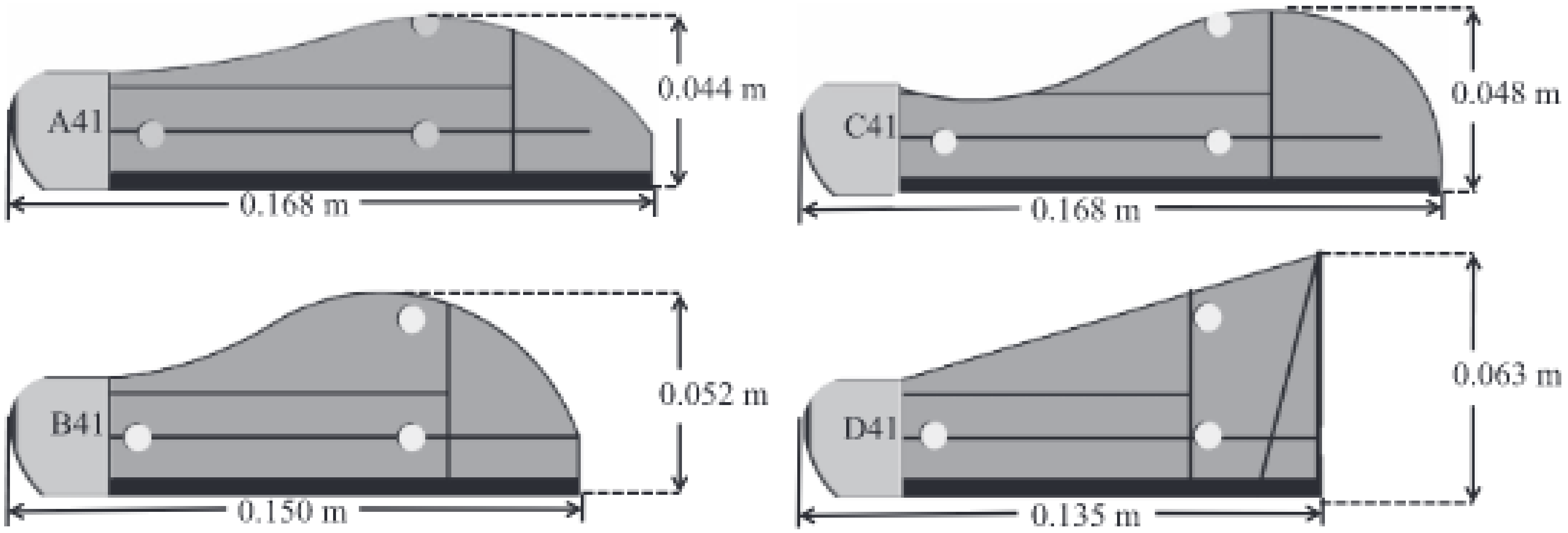

INTRINSIC EQUILIBRIUM OF AUTOROTATION

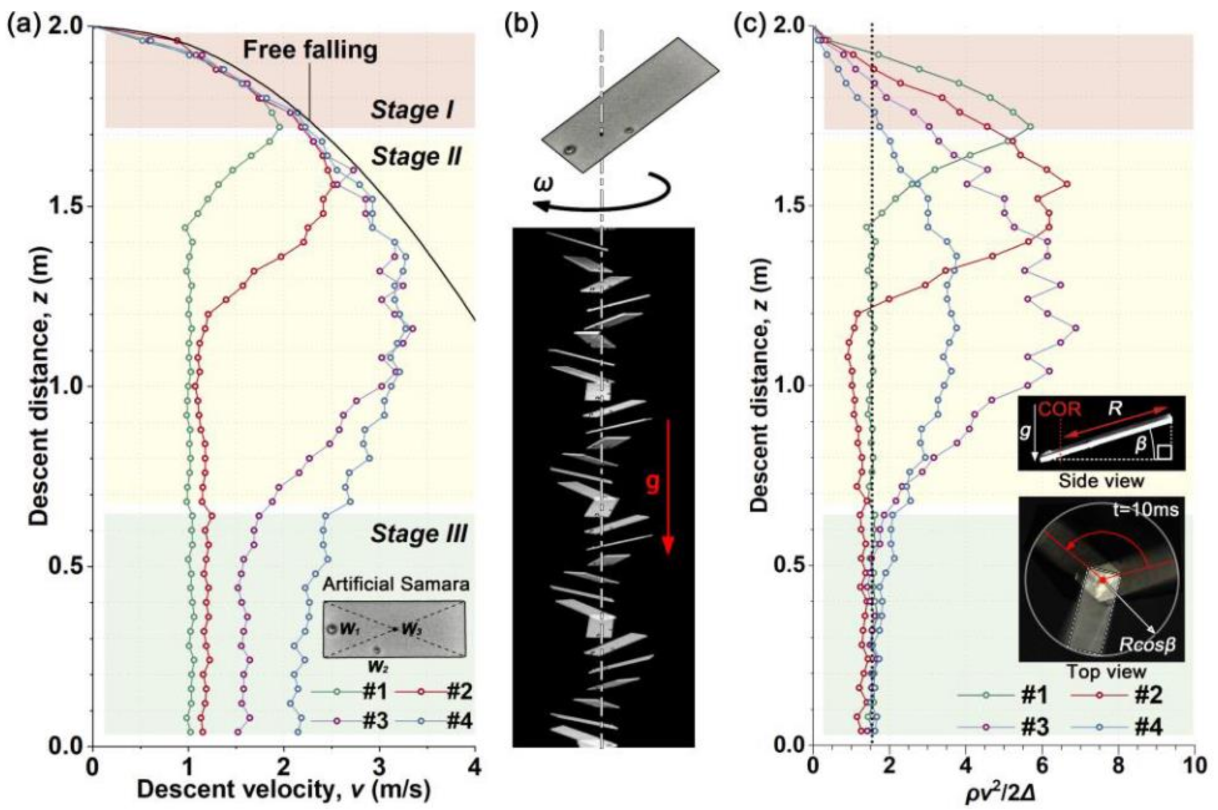

- Freefall Biological and Artificial Samara Tests
- Generalized Parameter: $\frac{\rho v^2}{2\Delta}$
  - Dynamic Pressure: $\frac{1}{2}\rho v^2$
  - Disk Loading: Δ
- Stages
  - Stage 1: Free Fall
  - Stage 2: Transition—Subjected to Crosswind
  - Stage 3: Auto-rotation

INTRINSIC EQUILIBRIUM OF AUTOROTATION

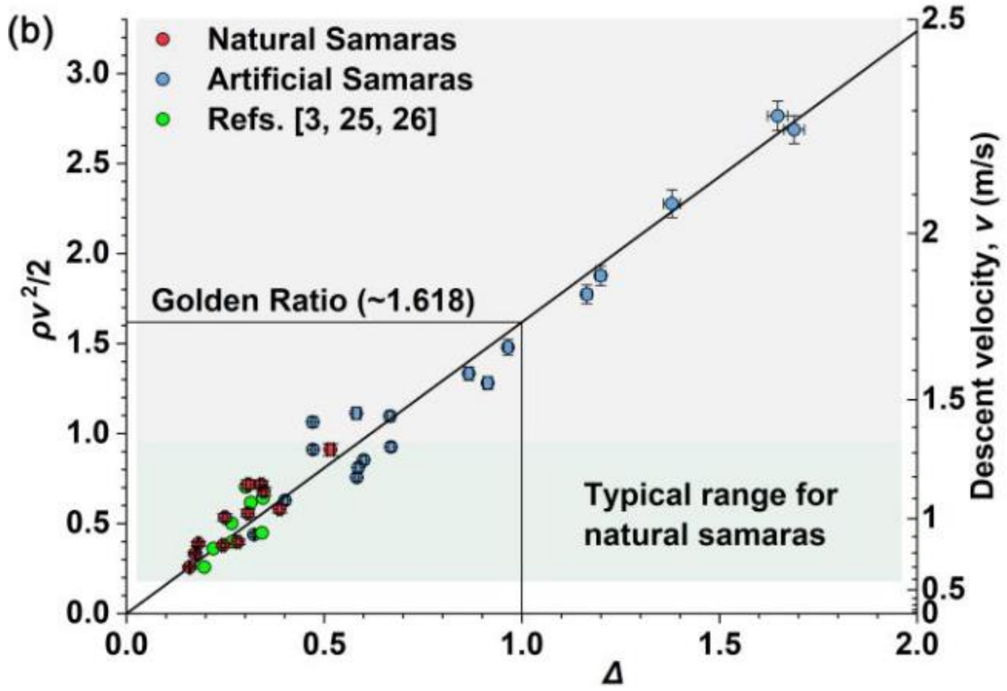

- Transition Stage: Low disk-loading, high dynamic pressure
- Steady-State:
  - Disk-loading and Dynamic pressure balanced: $\frac{\rho v^2}{2\Delta} \sim \frac{1}{C_L}$
  - Parameter: $\frac{1}{C_L} \sim 1.618 \Rightarrow C_L \sim .618$
- Coning Angle (θ) dependent on the torque generated by the lift and drag on the blade
- Increasing angular velocity $(\dot{\omega} > 0)$ causes the seed to flip and begin auto-rotation

STABILITY ANLYSIS

CONTROLS BASED MODEL

Development of a State Space Model to describe the dynamics of the samara seed through all phases of flight

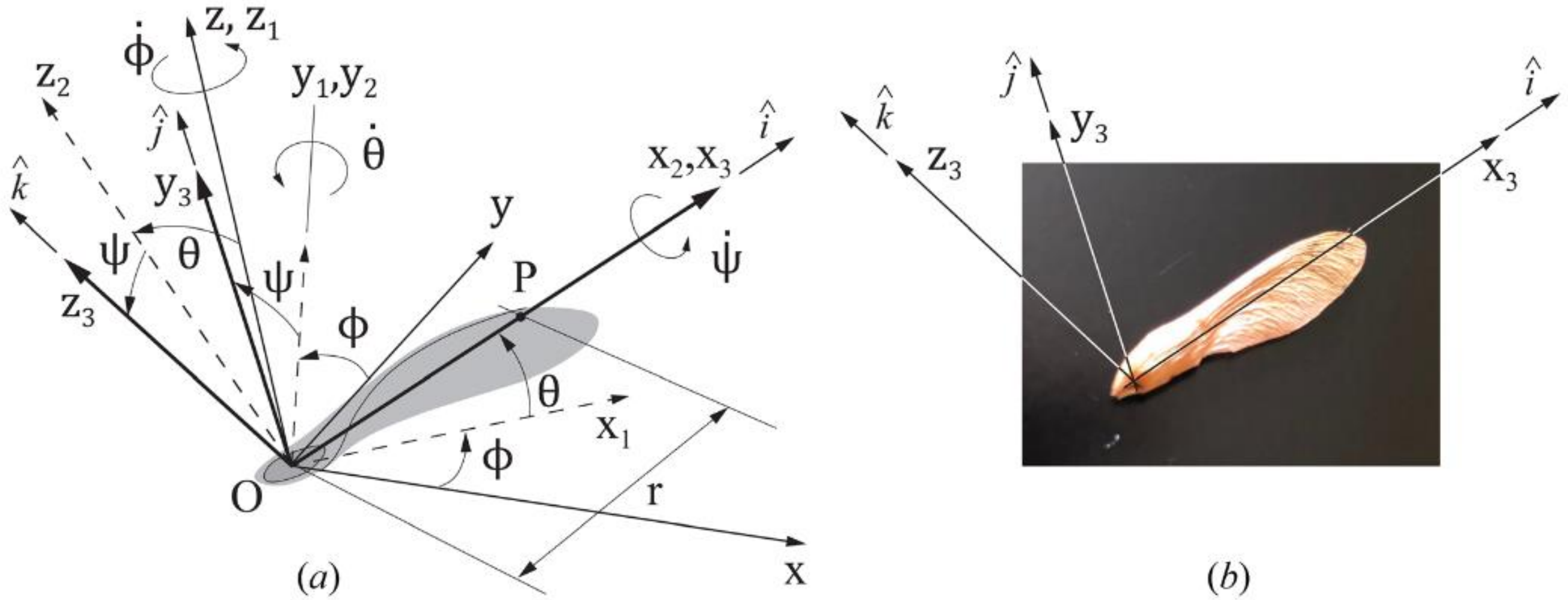

Fig. 1 Euler angle definition for a samara

EQUATIONS OF MOTION (EOM)

Term	Definition
$\dot{\Theta}$	Coning Rate
$\dot{\phi}$	Yaw Rate
ψ	Roll Angle
v_0	Vertical Descent Rate
m	Mass

$$\ddot{\theta}\cos\psi + \dot{\phi}^2 \sin\theta\cos\psi + 2\dot{\phi}\dot{\theta}\sin\psi - \ddot{\phi}\cos\theta\sin\phi = -M_{y_3}/I_{y_3 y_3}$$

$$\ddot{\theta}\sin\psi + \dot{\phi}^2 \sin\theta\cos\psi - 2\dot{\phi}\dot{\theta}\sin\psi + \ddot{\phi}\cos\theta\sin\phi = -M_{z_3}/I_{y_3 y_3}$$

$$\dot{v_0} = -g + \left(F_{y_3}\cos\theta\sin\phi\right)/m + \left(F_{z_3}\cos\theta\sin\phi\right)/m$$

STEADY STATE AUTOROTATION

Term	Definition
M_{y_3}	Moment about y_3 axis
M_{z_3}	Moment about z_3 axis
$I_{y_3 y_1}$	Moment of inertia about the y_3 y_1 axes
F_{y_3}	Force along the y_3 axis
F_{z_3}	Force along the z_3 axis

- Steady State: $\ddot{\theta} = \ddot{\phi} = \dot{\theta} = \dot{v}_0 = 0$
- Negligible Roll Rate

$$\dot{\phi}^2 \sin\theta \cos\theta \cos\psi = -M_{y_3}/I_{y_3 y_1}$$

$$\dot{\phi}^2 \sin\theta \cos\theta \sin\psi = -M_{z_3}/I_{y_3 y_1}$$

$$mg = F_{y_3} \sin\psi \cos\theta + F_{z_3} \cos\psi \cos\theta$$

LIFT AND DRAG

$$\boldsymbol{C_L(\alpha) = 2\pi \sin(\alpha)}$$
$$\boldsymbol{C_D(\alpha) = C_L(\alpha)\sin(\alpha) + C_{D_0}}$$

$$Tip\ Speed\ Ratio \stackrel{\text{def}}{=} \lambda = \frac{v_0}{r\dot{\phi}}$$

$$\frac{v_{0,e}}{0.9R\dot{\phi}_e} \leq \frac{v_{0,e}}{r\dot{\phi}_e} \leq \frac{v_{0,e}}{0.2R\dot{\phi}_e} \Rightarrow \frac{\lambda_e}{0.9} \leq \frac{v_{0,e}}{r\dot{\phi}_e} \leq \frac{\lambda_e}{0.2}$$

$$\boldsymbol{C_{D_0} \leq 4\pi\left(\sqrt{1+\left(\frac{\lambda_e}{0.9}\right)^2} + \frac{\left(\frac{\lambda_e}{0.9}\right)^2}{2\left(1+\left(\frac{\lambda_e}{0.9}\right)^2\right)} - 1\right)}$$

Blade Element Momentum Theory (BEM)

MONO-COPTER MODEL

MONOCOPTER MODEL USING UNSTEADY BEM THEORY

$$dT_{BET} = F_p dT_{MT} + \dot{v}_i dm_a$$

$$\dot{\boldsymbol{v}}_{\boldsymbol{i}} = \frac{\mathbf{1}}{\boldsymbol{dm}_{\boldsymbol{A}}}(\boldsymbol{dT}_{\boldsymbol{BET}} - \boldsymbol{F}_{\boldsymbol{P}}\,\boldsymbol{dT}_{\boldsymbol{MT}})$$

Term	Definition
dT_{BET}	Thrust Force via BET
F_p	Prandtl's Tip Loss Function
dT_{MT}	Thrust Force via *steady* momentum theory
v_i	Induced velocity at element
dm_a	Apparent Mass of Air moved by element

LIFT AND DRAG FORCES

$$dL = \frac{1}{2}\rho U^2 c C_L(\alpha) dx^b$$

$$dD = \frac{1}{2}\rho U^2 c C_D(\alpha) dx^b$$

Term	Definition
dL, dD	Lift and Drag Force
ρ	Air Density
U^2	Resultant local airflow velocity
c	Local wing Chord
$C_L(\alpha), C_D(\alpha)$	Lift and Drag Coefficients
α	Pitch Angle
dx^b	Blade Element Width

MOMENTUM THEORY THRUST

$$\dot{v}_i = \frac{1}{dm_A}\left(dT_{BET} - F_P\, dT_{MT}\right)$$

$$dT_{MT} = 2\rho dA v_i \sqrt{V_\infty^2 + 2V_\infty v_i \sin\alpha_d + v_i^2}$$

Term	Definition
dA	Annulus Area
V_∞	Free Stream Velocity
v_i	Induced Velocity Perpendicular to annulus and opposite to Thrust
α_d	Rotor Disk angle of attack, positive for flow incoming from above the rotor

PRANDTL TIP LOSS FUNCTION

$$\dot{v}_i = \frac{1}{dm_A}\left(dT_{BET} - F_P\, dT_{MT}\right)$$

$$F_p = \frac{2}{\pi}\arccos\left(e^{-f}\right)$$

$$f = \frac{N_b}{2}\left(\frac{R-r}{R\sin\phi}\right)$$

Term	Definition
F_p	Lift loss at wing-tip
f	*N/A*
N_b	Number of propeller blades
R	Total Radius of rotor
r	Blade element radial position
ϕ	Local inflow angle

APPARENT MASS

$$\dot{v}_i = \frac{1}{dm_A}(dT_{BET} - F_P\, dT_{MT})$$

$$dm_A = \frac{8}{3}\rho(r_2^3 - r_1^3)$$

Term	Definition
dm_A	Apparent Mass of Air Moved
ρ	Air Density
r_1, r_2	Annulus Inner and Outer Bound

MODEL SUCCESSES

- Model overall is successful at simulating the behavior of mono-copter
- $\dot{v}_i = \frac{1}{dm_A}(dT_{BET} - F_P\, dT_{MT})$
- Passive Stability: Disturbance causing pitch in the same direction increases airflow on the advancing side generating more thrust
- Critical Failure Mode: Wing-pitch oscillations

Thesis - Kai Pointing

TRANSITION BEHAVIOR OF SAMARAS USING IMAGE PROCESSING

TRACKING SAMARA SEED TRAJECTORIES VIA HIGH-SPEED IMAGING

- 3D scans of samara seeds illustrating the geometric characteristics
- High-speed imaging rig capable of mapping out the trajectory completely through all stages of flight
- Generated raw-data sets for 100 seeds
- Developed python code-base to extract positional data
- Transition-time extracted for all seeds

TRACKING SAMARA SEED TRAJECTORIES VIA HIGH-SPEED IMAGING

- Statistical analysis comparing various geometric properties to respective transition times
- Fine-tune data smoothing filters
- Improve transition-time extraction method
- Extract Dynamic Behavior

Experimental Setup & Procedure

PROPOSED METHODOLOGY

SETUP AND PROCEDURE

- Complete 3D scan of seed to extract geometric properties
- Semi automatic tether triggers the seed drop and the camera simultaneously
  - Mirrors provide front and bottom views
  - Single drop angle
- High-speed camera & built-in software track seed during descent
- Python algorithm: Raw-Data Processing using Image-Masking
  - Trajectory Extraction
  - Kinematic Response Extraction
  - Dynamic Response Extraction

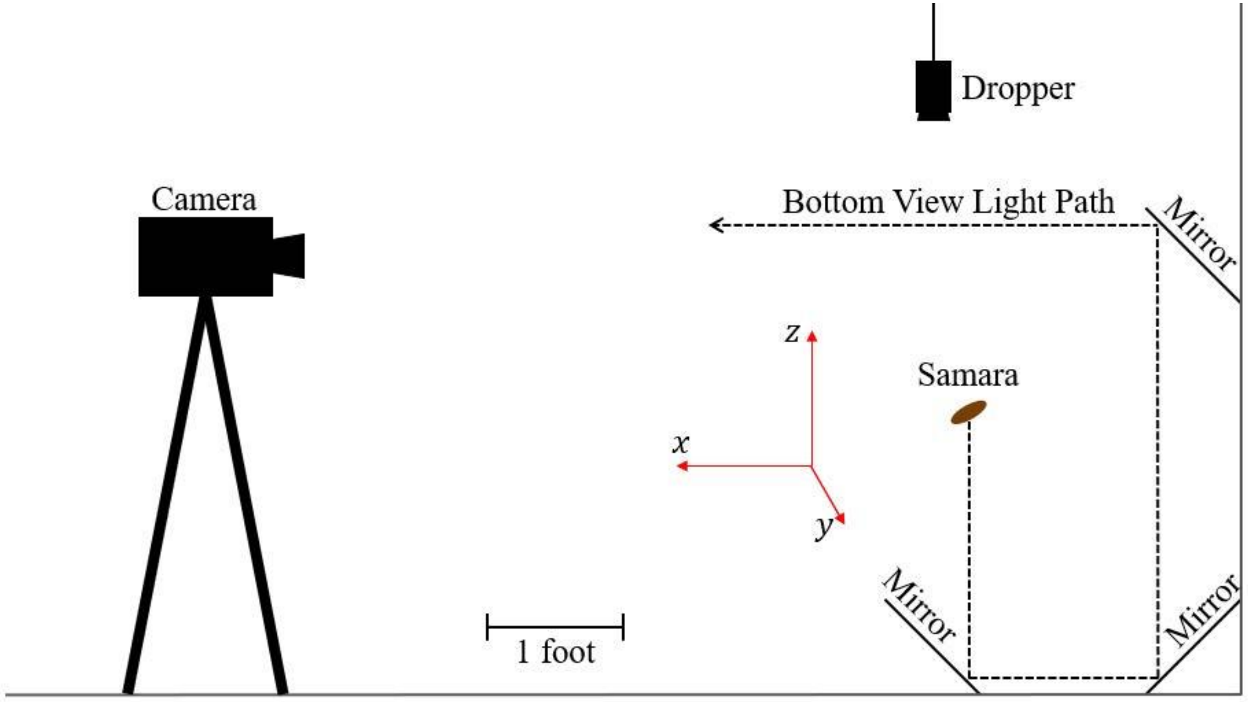

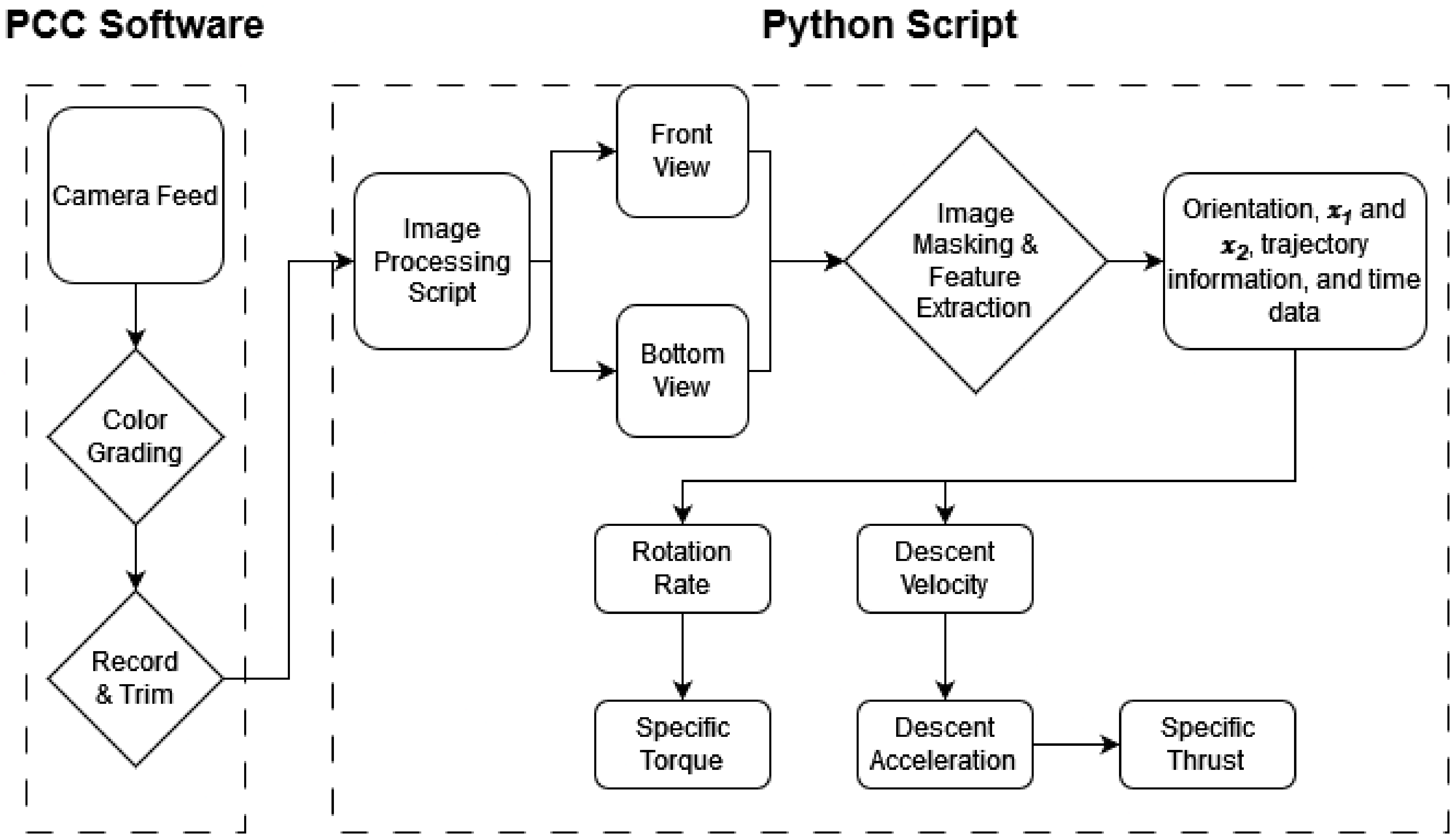
PCC Software
Python Script
Camera Feed
Color Grading
Record & Trim
Image Processing Script
Front View
Bottom View
Image Masking & Feature Extraction
Orientation, x_1 and x_2, trajectory information, and time data
Rotation Rate
Descent Velocity
Specific Torque
Descent Acceleration
Specific Thrust

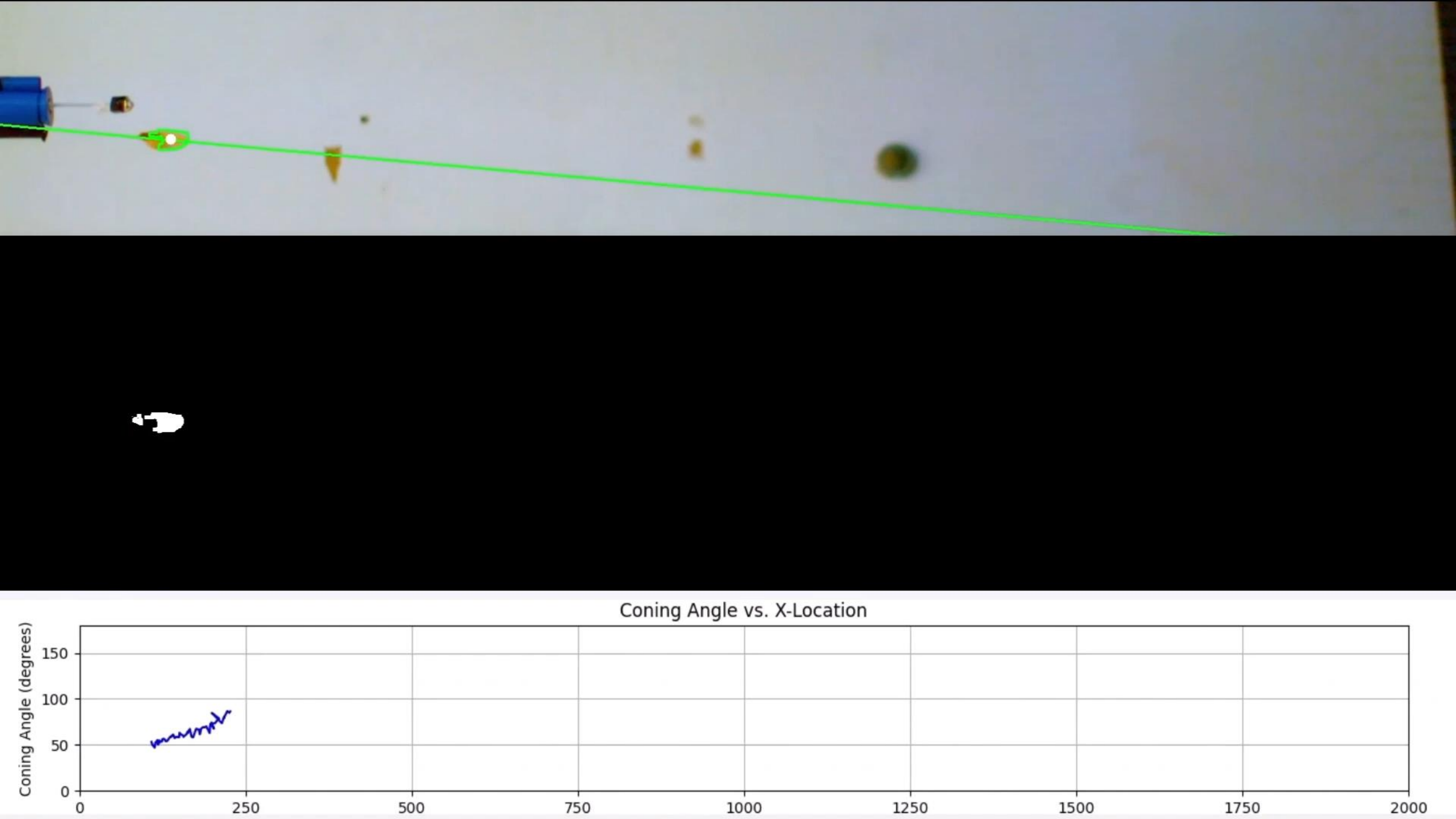
Coning Angle vs. X-Location
Coning Angle (degrees)
0
50
100
150
0
250
500
750
1000
1250
1500
1750
2000

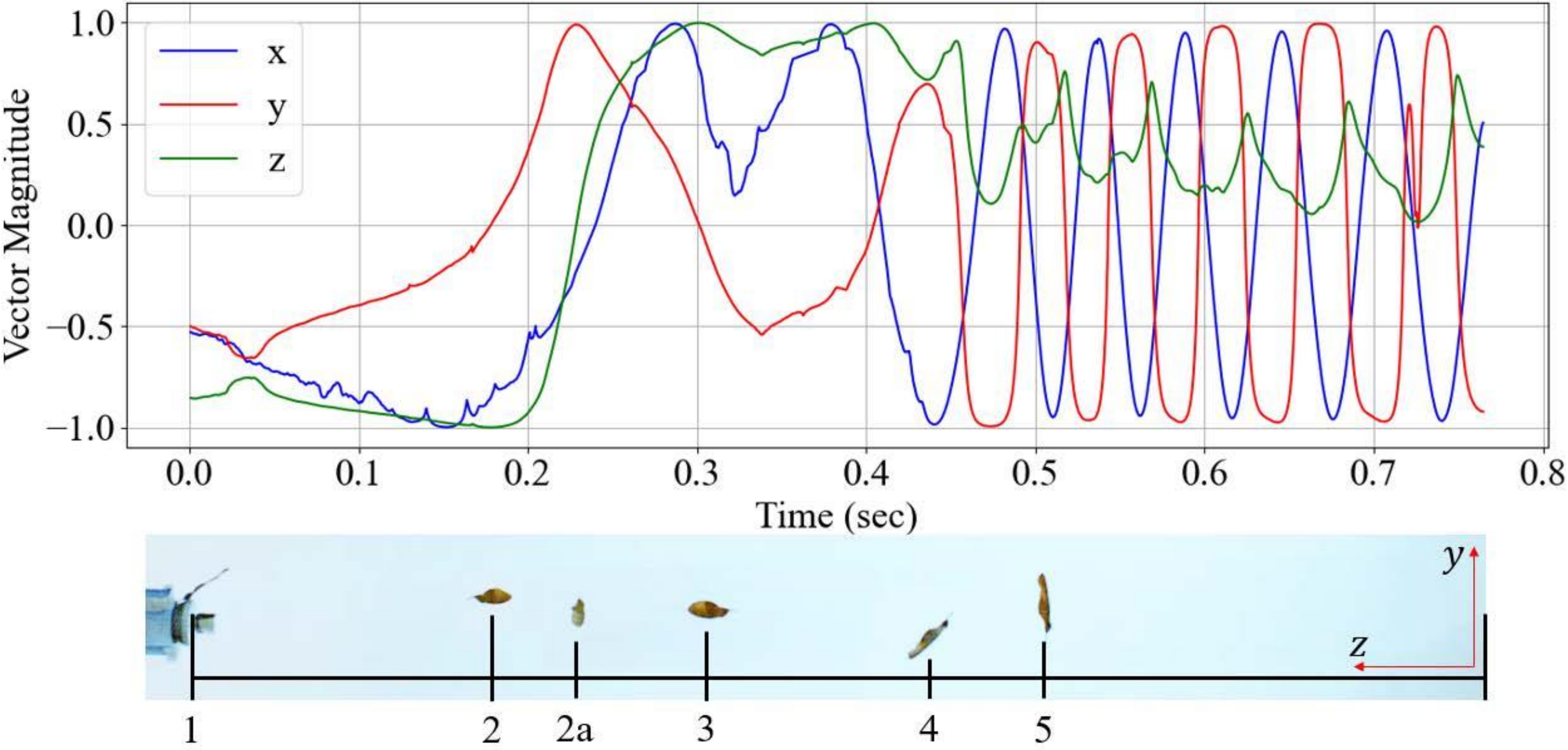

Vector Magnitude
Time (sec)
x
y
z
1.0
0.5
0.0
−0.5
−1.0
0.0
0.1
0.2
0.3
0.4
0.5
0.6
0.7
0.8
y
z
1
2
2a
3
4
5

SCOPE

MOTIVATIONAL QUESTIONS

- Do the single-bladed seeds undergoing auto-rotation truly support the widely accepted claim of seed dispersal?
- Is there any peculiar morphological or flight characteristics that make a minority number of seeds fly far distances?
- Determine the relationship between geometric and flight characteristics
- Investigate the kinematic and dynamic responses during steady-state
- Applications:
  - Biomimicry
  - Large Scale Terraforming via seed dispersal

STAGES OF FLIGHT

- Free Fall: Kinematics modeled by Free Fall
- Transition:
  - Time period between start of fall and the instant it begins steady-state rotation like a helicopter
  - Not the subject of most aerodynamic studies
- Steady-State:
  - Seed exhibits auto-rotation and lower descent velocity
  - Primary focus of most studies
- Initial attitude and form factor have a significant impact
- Small Aerodynamic Torque in the initial drop perturbed the seed in order to generate rotation

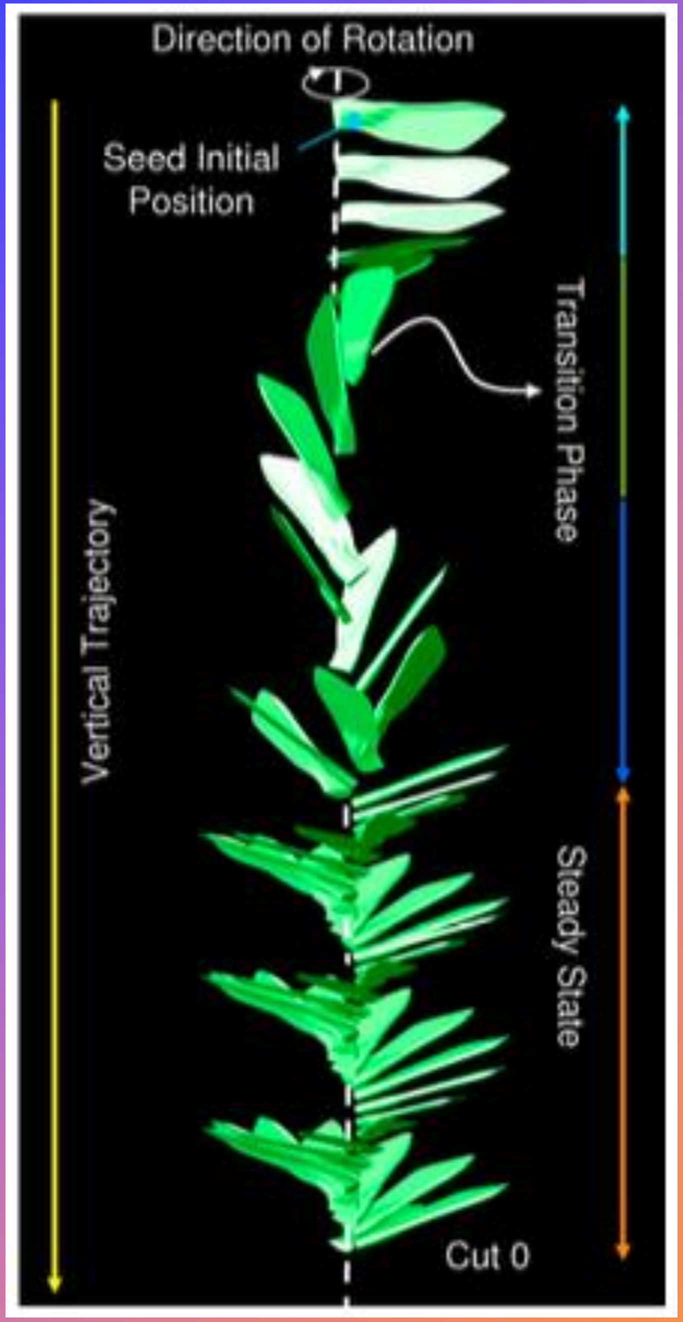

[Reference 14]

SUCCESS CRITERIA

- Complete Statistical Analysis of existing data-sets on transition time
- Develop robust method for extracting the kinematic and dynamic behaviors during steady-state descent
  - Analyze 3 seeds based on performance: Fast, Average, and Slow Transitioning
  - Extract Specific Thrust (S_{Thrust}) and Specific Torque (S_{Torque})
  - Complete statistical analysis of S_{Thrust} and S_{Torque}
  - Specifically look to extract parameters like C_L and C_D
  - Verify these process results against existing models for the auto-rotation stage
  - Extract the radius of precession & gyration
  - Evaluate EOM considering lateral motion of seed
- Numerically map out the transition regimes and apply appropriate models to analyze kinematic and dynamic behavior
  - Specifically look to extract parameters like C_L and C_D
  - Re-test smaller sample size: Create new Data-Set

WBS	TASK TITLE	TASK DESCRIPTION	SCHEDULED START	SCHEDULED FINISH	DURATION IN DAYS	W1 12/30	W2 1/6	W3 1/13	W4 1/20	W5 1/27	W6 2/3
1.0	**Statistical Analysis**		**01/02/25**	**01/20/25**	**13**						
1.1	Independent T Test	Evaluate Relationship between Transition Time and Geometric Parameters	01/03/25	01/09/25	5						
1.2	ANOVA Test	Compare Relationships between Transition Time and Geometric Parameters	01/10/25	01/16/25	5						
1.3	Geometric Trends	Extract Trends between various Geometric Parameters	01/17/25	01/21/25	3						
1.4	Identify Geometric Param	Identify Characteristic Predictor for Transition Time	01/17/25	01/21/25	3						
2.0	**Data Processing: Kinematic**	**Steady-State + Transition**	**01/22/25**	**02/12/25**	**16**						
2.1	Smoothing	Develop process for data smoothing	01/22/25	01/26/25	3						
2.2	Transition Time Extraction	Develop robust process for extracting transition time	01/26/25	02/05/25	8						
2.3	Rotation Rate Extraction	Develop Fourier-Transform process for extracting the rotation rate	02/01/25	02/12/25	8						
2.4	Coning Rate Extraction	Develop Fourier-Transform process for extracting the coning rate	02/01/25	02/12/25	8						
2.5	Descent Velocity Extraction	Apply smoothing to extract descent velocity (V_d)	01/22/25	02/12/25	16						

WBS	TASK TITLE	TASK DESCRIPTION	SCHEDULED START	SCHEDULED FINISH	DURATION IN DAYS	W7 2/10	W8 2/17	W9 2/24	W10 3/3	W11 3/10	W12 3/17	W13 3/24	W14 3/31	W15 4/7	W16 4/14	W17 4/21
3.0	**Data Processing: Dynamic**	**Steady-State Analysis**	**02/14/25**	**04/30/25**	**54**											
3.1	Thrust & Torque Extraction	Extract Specific Thrust and Torque (S_{Thrust} and S_{Torque})	02/14/25	02/21/25	6											
3.2	Disk Loading Computation	Develop process for computing disk-loading	02/22/25	02/25/25	2											
3.3	Induced Velocity Extraction	Develop algorithm for computing induced velocity (V_i) at each time-step	02/26/25	03/17/25	14											
3.4	(V_i) Verification	Compare V_i to V_D	03/15/25	03/20/25	4											
3.5	Identify Wake Flow	Determine appropriate wake-flow model and verify against existing model	03/15/25	03/20/25	4											
3.6	Lift & Drag Extraction: Thin Airfoil	Extract the Coefficients of Lift and Drag (C_L and C_D) using thin air-foil assumption	03/21/25	04/10/25	15											
3.7	Comparison	Compare Thin-Airfoil model results to intrinsic equilbrium results	03/21/25	04/10/25	15											
3.8	Extract Gyration Radius	Compute the radius of gyration/radius of precession	04/10/25	04/15/25	4											
3.9	Develop Equations of Motion	Develop Equations of Motion incorporating radius of precession in SIMULINK	04/15/25	04/30/25	12											

STATISTICAL ANALYSIS

- Independent samples t-test
  - Define two distinct groups based on morphology
  - Parameters: Mass, Area, mg/A
- Analysis of Variance (ANOVA) test
  - Define multiple distinct groups based on morphology
  - Parameters: Mass, Span, Chord
- Determine statistical significance of relationships between parameters and transition time

STEADY-STATE

- Apply smoothing methods to eliminate noise in data
- Develop robust method for extracting rotation rate
  - Current is based on peak-to-peak data
  - Use Fourier Transform to extract Rotation Rate
- Evaluate S_{Thrust} and S_{Torque}

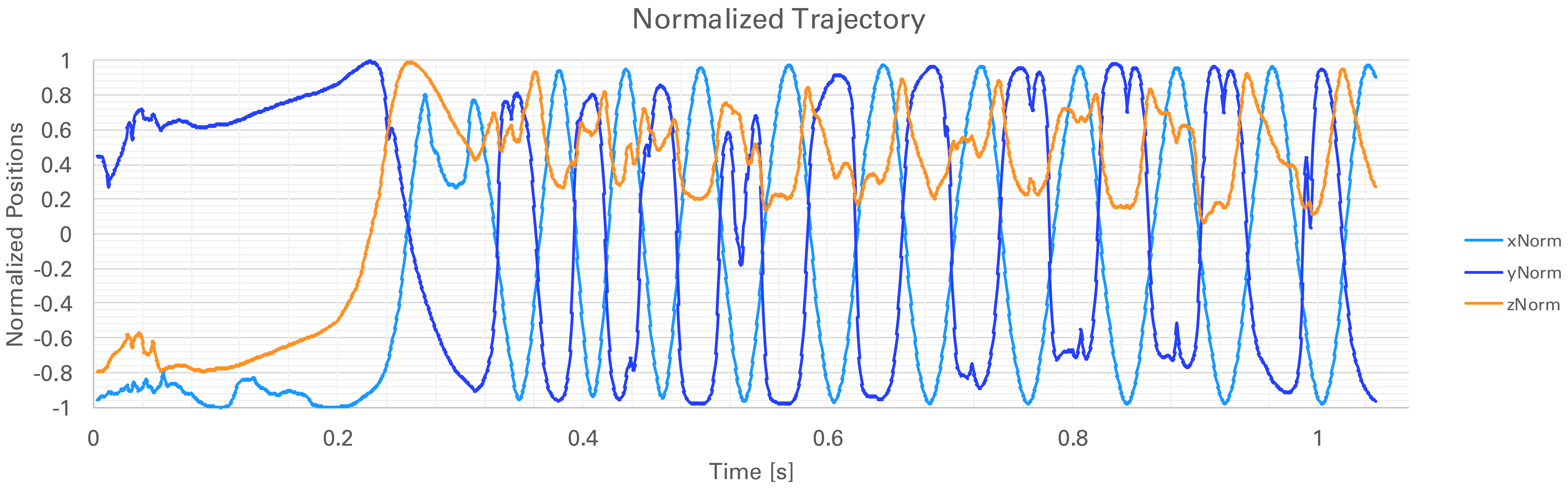

STEADY-STATE

- Compute C_L and C_D
  - Compare Controls Model to Intrinsic Auto-Rotation Model
  - $C_L(\alpha) = 2\pi \sin(\alpha)\,,\ C_{D_0} \leq 4\pi\left(\sqrt{1+\left(\frac{\lambda_e}{0.9}\right)^2} + \frac{\left(\frac{\lambda_e}{0.9}\right)^2}{2\left(1+\left(\frac{\lambda_e}{0.9}\right)^2\right)} - 1\right)$
  - $C_D \sim 5.68, C_L \sim .618$
- Compute induced velocity via
  - $\dot{v}_i = \frac{1}{dm_A}(dT_{BET} - F_P\, dT_{MT})$
  - Verify result using Windmill-Brake state model: $v_i < v_d$
- Develop EOM to account for Radius of Gyration in Simulink

POTENTIAL FUTURE WORK

- Experimental Testing
  - Repeated n number of tests for s samples of seeds
  - Statistical analysis of average and variance across both tests and samples
- Vertical Wind Tunnel Testing
  - Analyze sample aerodynamics using codebase
  - Develop artificial samara with similar mass and material properties
  - Validate results using vertical wind-tunnel testing
    - Hover seeds at appropriate speed
    - Compare performance of natural samara to artificial samara

THANK YOU

Shashwat Sparsh

ssparsh@calpoly.edu

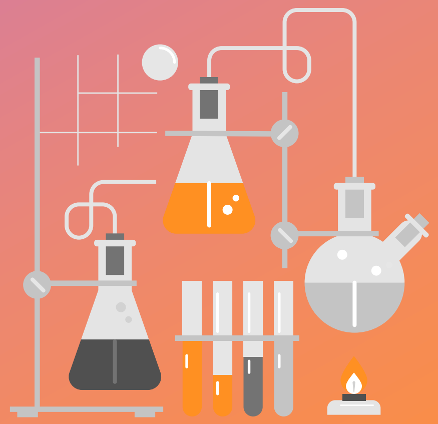

REFERENCES

REFERENCES (1/4)

1. Bai, S., He, Q., & Chirarattananon, P. (2022a). A bioinspired revolving-wing drone with passive attitude stability and efficient hovering flight. *Science Robotics*, *7*(66), eabg5913. https://doi.org/10.1126/scirobotics.abg5913
2. Bai, S., He, Q., & Chirarattananon, P. (2022b). A bioinspired revolving-wing drone with passive attitude stability and efficient hovering flight. *Science Robotics*, *7*(66), eabg5913. https://doi.org/10.1126/scirobotics.abg5913
3. Chen, T., & Lan, S. (2022). Numerical analysis of dynamic stability of falling maple samaras. *Acta Mechanica Sinica*, *38*(12), 322111. https://doi.org/10.1007/s10409-022-22111-x
4. Dorfling, J., & Rokhsaz, K. (2015). Constrained and Unconstrained Propeller Blade Optimization. *Journal of Aircraft*, *52*(4), 1179–1188. https://doi.org/10.2514/1.C032859
5. G, Y., M.V., S. R., & Gopalan, J. (2023, January 23). Investigation of wake flow around the single-winged autorotating seed using PIV. *AIAA SCITECH 2023 Forum*. AIAA SCITECH 2023 Forum, National Harbor, MD & Online. https://doi.org/10.2514/6.2023-1025
6. Heyson, H. H. (n.d.). *X+ MOMENTUMANALYSIS OF HELICOPTERS ANDAUTOGYROSININCLINED DESCENT, WITH COMMENTS ON OPERATIONALRESTRICTION3*.

REFERENCES (2/4)

7. Inoue, O., Hattori, Y., Akiyama, K., Inoue, O., Hattori, Y., & Akiyama, K. (1997, June 29). Calculations of vortex ring states and autorotation in helicopter rotor flow fields. *28th Fluid Dynamics Conference*. 28th Fluid Dynamics Conference, Snowmass Village,CO,U.S.A. https://doi.org/10.2514/6.1997-1847
8. Jung, B., & Rezgui, D. (2023, January 23). Flight Performance of an Autorotating Samara with varying windspeed. *AIAA SCITECH 2023 Forum*. AIAA SCITECH 2023 Forum, National Harbor, MD & Online. https://doi.org/10.2514/6.2023-2111
9. Jung, B. K., & Rezgui, D. (2024). Experimental study into the effects of pitch and coning angles on the flight performance of the natural samara. *Royal Society Open Science*, *11*(9), 240758. https://doi.org/10.1098/rsos.240758
10. Kang, S., Wang, J., & Shan, J. (2015). Dynamics analysis and simulation for the invisible monowing rotorcraft. *The 27th Chinese Control and Decision Conference (2015 CCDC)*, 4029–4034. https://doi.org/10.1109/CCDC.2015.7162628
11. Lee, I., & Choi, H. (2017). Flight of a falling maple seed. *Physical Review Fluids*, *2*(9), 090511. https://doi.org/10.1103/PhysRevFluids.2.090511
12. Lee, S. J., Lee, E. J., & Sohn, M. H. (2014). Mechanism of autorotation flight of maple samaras (Acer palmatum). *Experiments in Fluids*, *55*(4), 1718. https://doi.org/10.1007/s00348-014-1718-4

REFERENCES (3/4)

13. McConnell, J., & Das, T. (2023). Control Oriented Modeling, Experimentation, and Stability Analysis of an Autorotating Samara. *Journal of Dynamic Systems, Measurement, and Control*, *145*(6), 061004. https://doi.org/10.1115/1.4062438
14. Ng, M., Tang, E., Soh, G. S., & Foong, S. (2020). SHIFT: Selective Heading Image for Translation An onboard monocular optical flow estimator for fast constantly rotating UAVs. *2020 IEEE International Conference on Robotics and Automation (ICRA)*, 8525–8531. https://doi.org/10.1109/ICRA40945.2020.9197073
15. Niu, P., Atkins, M. D., Liu, Y., Li, M., Lu, T. J., & Kim, T. (n.d.). *Intrinsic Equilibrium of Stably Autorotating Samaras*.
16. Niu, P. X., Atkins, M. D., Liu, Y. Y., Lu, T. J., & Kim, T. (2022). Kinematic responses of an autorotating samara to concentrated crosswind. *Physics of Fluids*, *34*(11), 111912. https://doi.org/10.1063/5.0125421
17. Obradovic, B., Ho, G., Barto, R., Fregene, K., & Sharp, D. (2012, August 13). A Multi-Scale Simulation Methodology for the Samarai Monocopter ?UAV. *AIAA Modeling and Simulation Technologies Conference*. AIAA Modeling and Simulation Technologies Conference, Minneapolis, Minnesota. https://doi.org/10.2514/6.2012-5012
18. Pantel, H., Falissard, F., & Dufour, G. (2024). Assessment of Reynolds-Averaged Navier–Stokes/Blade Element Theory Body Force Method for Propeller Modeling. *AIAA Journal*, *62*(2), 758–775. https://doi.org/10.2514/1.J063302
19. Pratumnopharat, P., & Leung, P. S. (2011). Validation of various windmill brake state models used by blade element momentum calculation. *Renewable Energy*, *36*(11), 3222–3227. https://doi.org/10.1016/j.renene.2011.03.027

REFERENCES (4/4)

20. Ulrich, E., Grauer, J., Pines, D., Hubbard, J., & Humbert, S. (2010, August 2). Identification of a Robotic Samara Aerodynamic/Multi-Body Dynamic Model. *AIAA Atmospheric Flight Mechanics Conference*. AIAA Atmospheric Flight Mechanics Conference, Toronto, Ontario, Canada. https://doi.org/10.2514/6.2010-8233
21. Ulrich, E. R., Faruque, I., Grauer, J., Pines, D. J., Humbert, J. S., & Hubbard, J. E. (2010). Control Model for Robotic Samara: Dynamics About a Coordinated Helical Turn. *Journal of Guidance, Control, and Dynamics*, *33*(6), 1921–1927. https://doi.org/10.2514/1.50878
22. Ulrich, E. R., & Pines, D. J. (2012). Effects of Planform Geometry on Mechanical Samara Autorotation Efficiency and Rotational Dynamics. *Journal of the American Helicopter Society*, *57*(1), 1–10. https://doi.org/10.4050/JAHS.57.012003
23. Ulrich, E. R., Pines, D. J., & Humbert, J. S. (2010). From falling to flying: The path to powered flight of a robotic samara nano air vehicle. *Bioinspiration & Biomimetics*, *5*(4), 045009. https://doi.org/10.1088/1748-3182/5/4/045009
24. Varshney, K., Chang, S., & Wang, Z. J. (2012). The kinematics of falling maple seeds and the initial transition to a helical motion. *Nonlinearity*, *25*(1), C1–C8. https://doi.org/10.1088/0951-7715/25/1/C1
25. Venkatakrishnan, L., Majumdar, S., Subramanian, G., Bhat, G. S., Dasgupta, R., & Arakeri, J. (Eds.). (2021). *Proceedings of 16th Asian Congress of Fluid Mechanics*. Springer Singapore. https://doi.org/10.1007/978-981-15-5183-3

APPENDIX

STABILITY MODEL DETAILS

$$dF_{y_3} = \frac{1}{2}\rho w(r)||\mathbf{U}_\infty||^2(\sin\alpha\, C_L(\alpha) - \cos\alpha\, C_D(\alpha))dr$$
$$dF_{z_3} = \frac{1}{2}\rho w(r)||\mathbf{U}_\infty||^2(\cos\alpha\, C_L(\alpha) + \sin\alpha\, C_D(\alpha))dr$$

$$F_{y_3} = \int_{r_0}^{r_f} dF_{y_3}, \qquad F_{z_3} = \int_{r_0}^{r_f} dF_{z_3}$$

$$M_{z_3} = \int_{r_0}^{r_f} r\, dF_{y_3}, \quad M_{y_3} = -\int_{r_0}^{r_f} r\, dF_{z_3}$$

$$I_{y_3 y_3} = \frac{1}{3} fmR^2$$

$$||U_\infty||^2 = r^2\dot{\phi}^2\cos^2\theta + (r\dot{\theta} + v_0\cos\theta)^2$$

$$\sin\alpha = [-v_0\cos\theta\cos\psi + r(\dot{\phi}\cos\theta\sin\psi - \dot{\theta}\cos\psi)]/||U_\infty||$$

$$\cos\alpha = [v_0\cos\theta\sin\psi + r(\dot{\phi}\cos\theta\cos\psi + \dot{\theta}\sin\psi)]/||U_\infty||$$

$$M_{y_3} = -I_{y_3 y_3}\,\dot{\phi}^2 \sin\theta \cos\theta \cos\psi$$

$$= -\frac{1}{2}\rho\,\dot{\phi}\cos^2\theta\int_{r_0}^{r_f} r^3\, w(r)\sqrt{1+\left(\frac{\lambda}{\chi}\right)^2}$$

$$\left[\left(\frac{\lambda}{\chi}C_L(\alpha)+C_D(\alpha)\right)\sin\psi\right.$$

$$\left.-\left(C_L(\alpha)-\frac{\lambda}{\chi}C_D(\alpha)\right)\cos\psi\right]dr$$

$$M_{z_3} = I_{y_3 y_3}\, \dot{\phi}^2 \sin\,\theta \cos\,\theta \sin\,\psi$$

$$= \frac{1}{2} \rho\, \dot{\phi} \cos^2 \theta \int_{r_0}^{r_f} r^3\, w(r) \sqrt{1 + \left(\frac{\lambda}{\chi}\right)^2}$$

$$\left[\left(C_L(\alpha) + \frac{\lambda}{\chi} C_D(\alpha)\right) \sin\,\psi\right.$$

$$\left. + \left(\frac{\lambda}{\chi} C_L(\alpha) - C_D(\alpha)\right) \cos\,\psi\right] dr$$

$$mg = \frac{1}{2}\rho\,\dot{\phi}\,\cos^2\theta\int_{r_0}^{r_f} r^2\,w(r)\sqrt{1+\left(\frac{\lambda}{\chi}\right)^2}\cdot$$
$$\left[\left(-\frac{\lambda}{\chi}C_L(\alpha)+C_D(\alpha)\right)\sin\,\psi\right.$$
$$\left.+\left(C_L(\alpha)+\frac{\lambda}{\chi}C_D(\alpha)\right)\cos\,\psi\right]dr$$

MODEL LIMITATIONS AND SUCCESSES

- Negligible Roll Angle
- Simple thin Airfoil Model
- Model does not account for the LEV but still simulates the behavior for Low Reynolds number flows
- **Solving the equations of motion indicates that $C_{D_0} \neq 0$ even when $(\psi = 0)$ indicating it is crucial to the auto-rotation equilibrium**
- Numerical solutions to the full state-space model encounter convergence issues

TASK LIST SUMMARIZED

TASK LIST

- Improve data-processing algorithm to reduce noise
- Complete statistical analysis of transition-time to geometric parameter to identify trends
- Develop algorithm to extract kinematic and dynamic parameters through transition and steady-state
  - Improve transition-time extraction algorithm
  - Specific Thrust and Torque
  - Utilize Fourier Transform to identify coning angle and rotation rate
  - $\dot{v}_i = \frac{1}{dm_A}(dT_{BET} - F_P\, dT_{MT})$
  - Extract C_L and C_D

TASK LIST

- Extract C_L and C_D
  - Thin Airfoil Model
    - $C_D(\alpha) = C_L(\alpha)\sin(\alpha) + C_{D_0}$
    - $C_{D_0} \leq 4\pi\left(\sqrt{1+\left(\frac{\lambda_e}{0.9}\right)^2} + \frac{\left(\frac{\lambda_e}{0.9}\right)^2}{2\left(1+\left(\frac{\lambda_e}{0.9}\right)^2\right)} - 1\right)$
  - Intrinsic Auto-Rotation Model
    - $\frac{\rho v^2}{2\Delta} \sim \frac{1}{C_L} \sim 1.618 \Rightarrow C_L \sim .618$
- Compare Model Results

TRANSITION

- Compute C_L and C_D via Controls Model
  - $C_L(\alpha) = 2\pi\sin(\alpha)\,,\; C_{D_0} \leq 4\pi\left(\sqrt{1+\left(\frac{\lambda_e}{0.9}\right)^2} + \frac{\left(\frac{\lambda_e}{0.9}\right)^2}{2\left(1+\left(\frac{\lambda_e}{0.9}\right)^2\right)} - 1\right)$
- Compute Induced Velocity using BEM model
  - $\dot{v}_i = \frac{1}{dm_A}\left(dT_{BET} - F_P\, dT_{MT}\right)$
  - Determine Wake-Flow State
    - Windmill-Brake vs Vortex-Ring
    - $v_i < v_d$ or $v_i > v_d$
    - $\left|\frac{v_i}{v_d}\right| > 1$ or $\left|\frac{v_i}{v_d}\right| < 1$

Experimental Setup & Procedure

PROPOSED METHODOLOGY

SETUP AND PROCEDURE

- Complete 3D scan of seed to extract geometric properties
- Semi automatic tether triggers the seed drop and the camera simultaneously
  - Mirrors provide front and bottom views
  - Single drop angle
- High-speed camera & built-in software track seed during descent
  - Phantom TMX 5010
  - Orthographic projections of seeds
  - Framerate: 5000Hz
- Python algorithm processes data for kinematics and dynamics

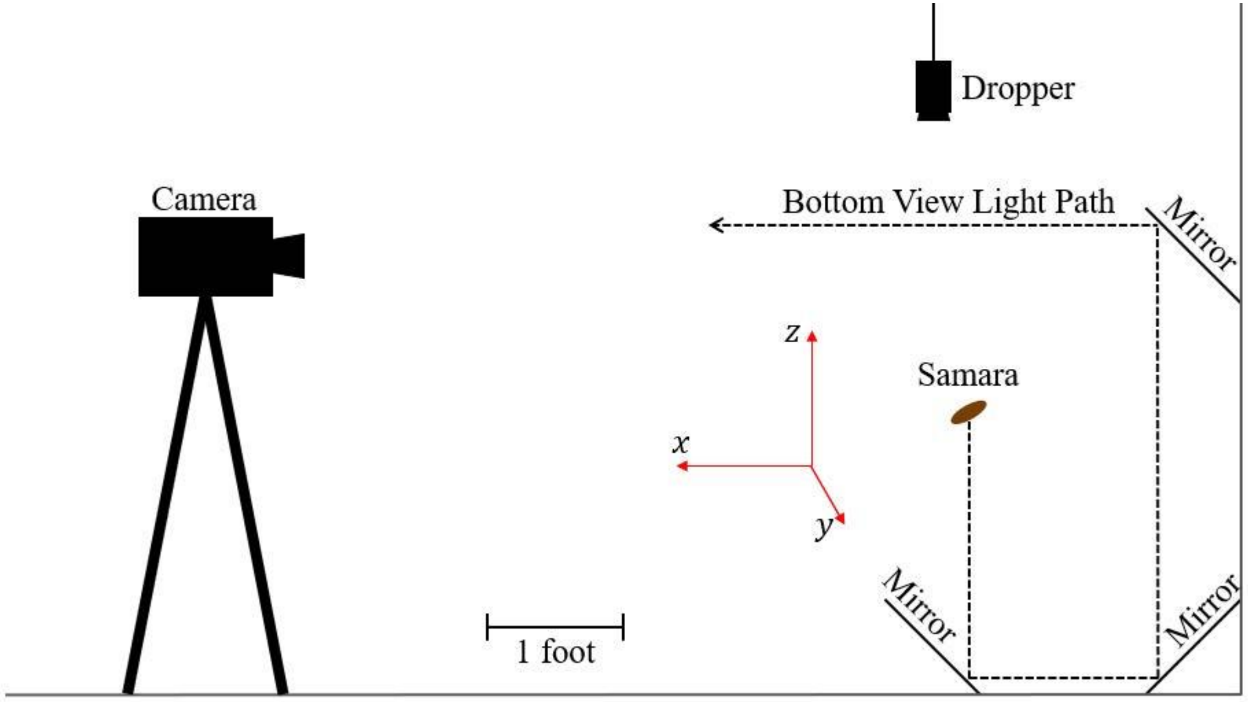

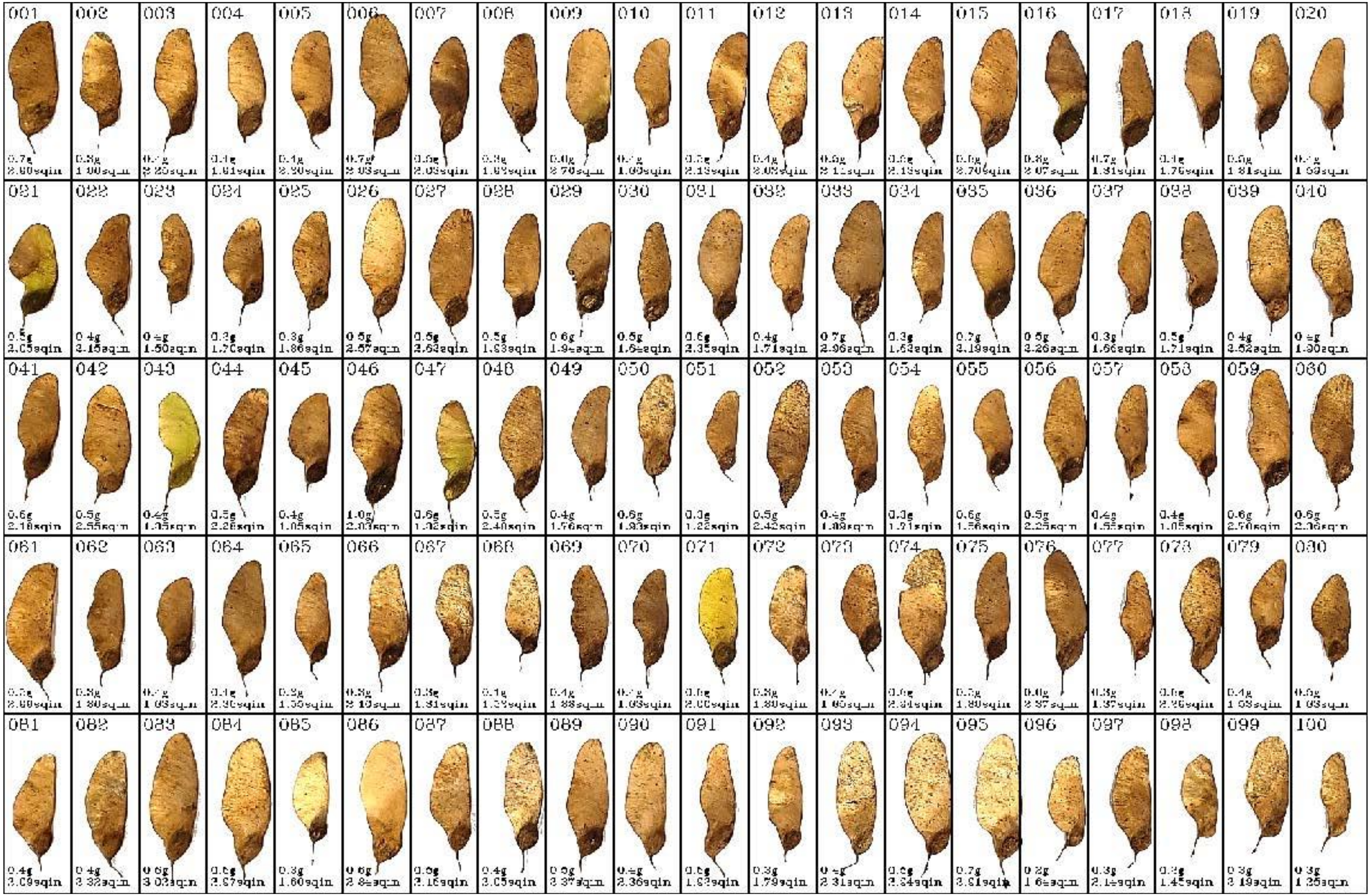
001
002
003
004
005
006
007
008
009
010
011
012
013
014
015
016
017
018
019
020
021
022
023
024
025
026
027
028
029
030
031
032
033
034
035
036
037
038
039
040
041
042
043
044
045
046
047
048
049
050
051
052
053
054
055
056
057
058
059
060
061
062
063
064
065
066
067
068
069
070
071
072
073
074
075
076
077
078
079
080
081
082
083
084
085
086
087
088
089
090
091
092
093
094
095
096
097
098
099
100

GEOMETRIC AXIS

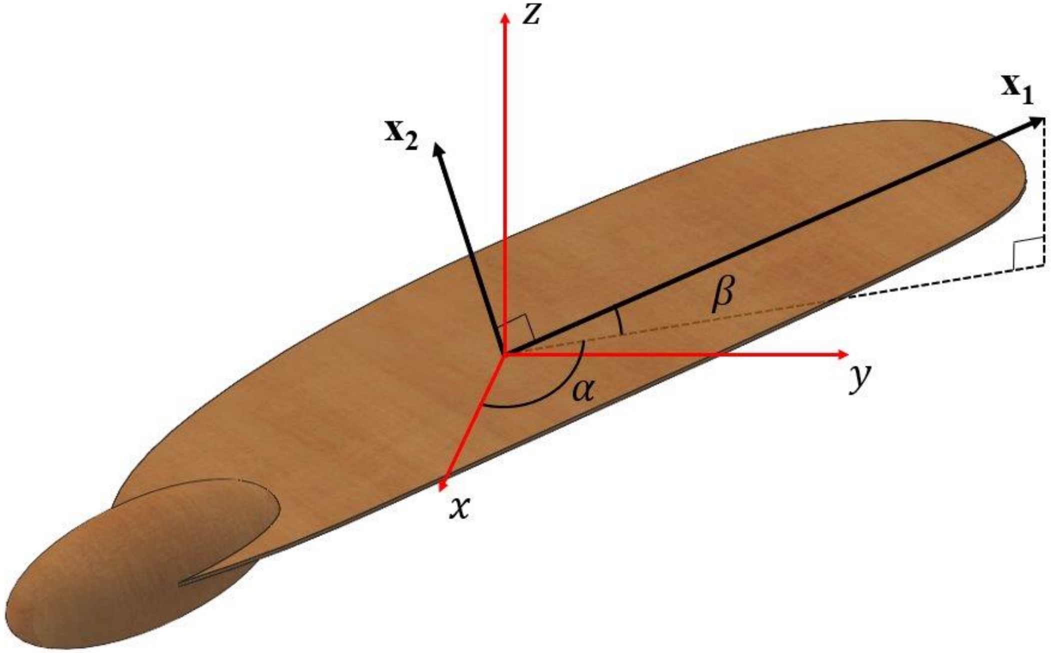

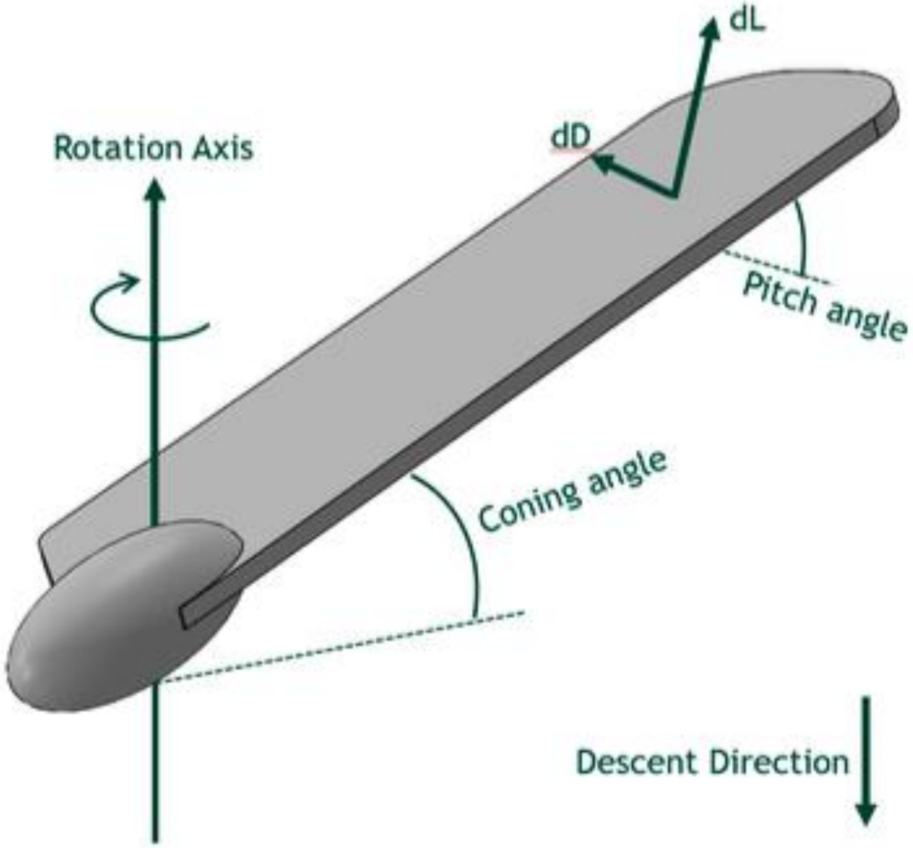

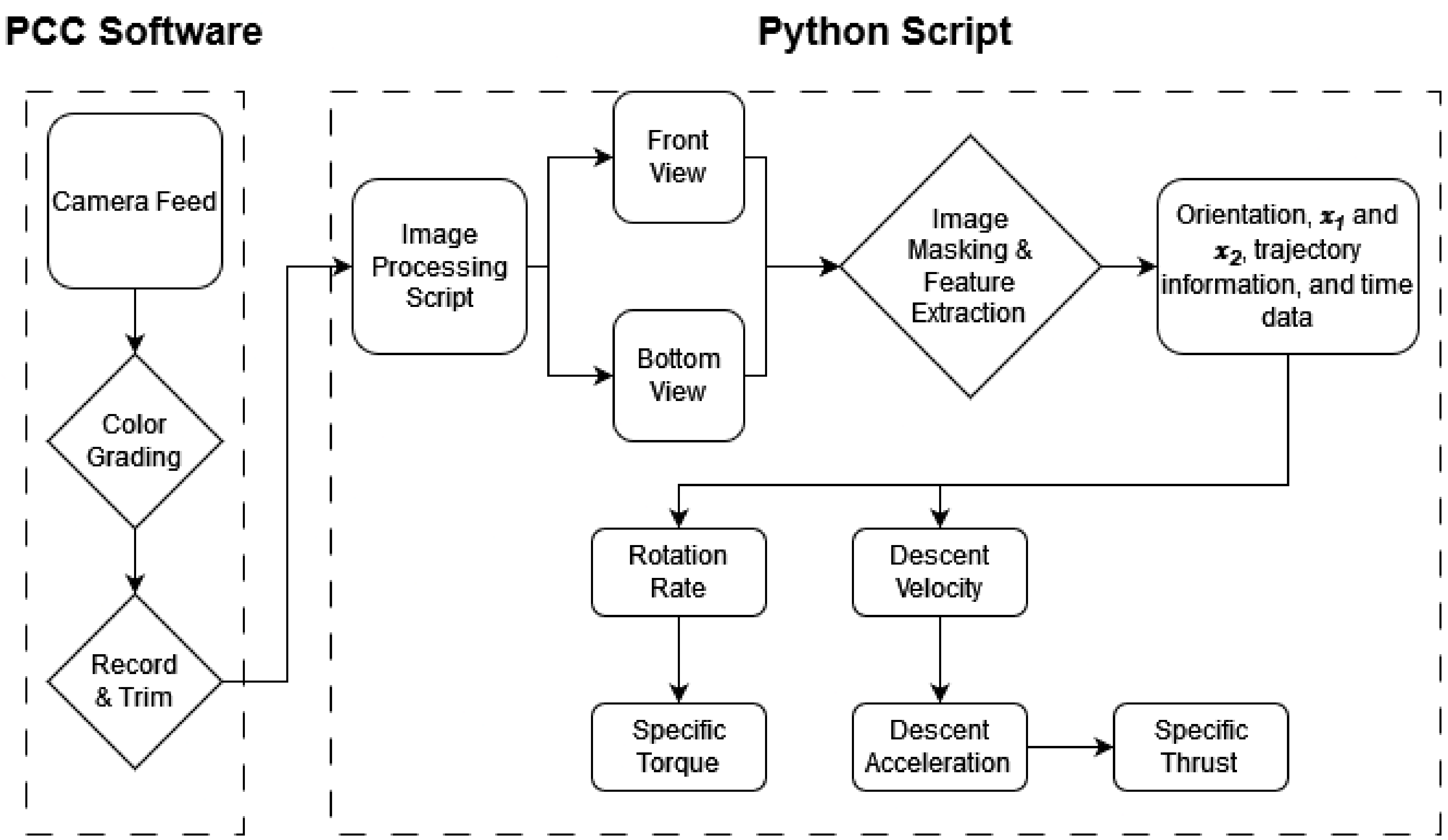
PCC Software
Python Script
Camera Feed
Color Grading
Record & Trim
Image Processing Script
Front View
Bottom View
Image Masking & Feature Extraction
Orientation, x_1 and x_2, trajectory information, and time data
Rotation Rate
Descent Velocity
Specific Torque
Descent Acceleration
Specific Thrust

PYTHON SCRIPT

- Libraries
  - Scipy and Numpy
  - Tsmoothie
  - Pandas
  - OpenCV
    - Create ellipse mask over seed
    - Extract position vectors (x, y, z) from ellipse
- Data Processing
  - Compute Descent Speed by referencing z position over time
    - Apply Kalman Filter to smooth out velocity data and reduce noise
  - Compute Acceleration by differencing velocity data over timestep
  - Compute Thrust by summing forces

FEATURE EXTRACTION

- Blur Out Background
- Convert to Binary Image
- Create contour fit using binary image
- Fit ellipse over contour
- Track ellipse points

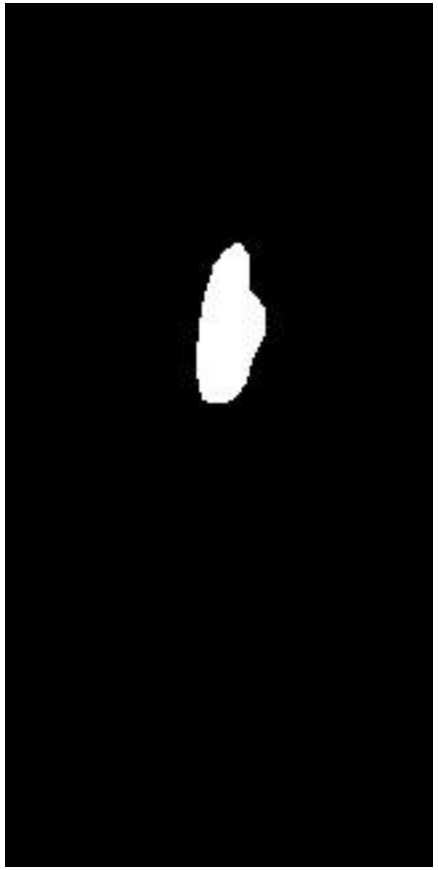

CONTOUR AND ELLIPSE FIT

ORIENTATION EXTRACTION

- Compute an Angle parameter from the front and bottom views
- Range of 0-180 degrees

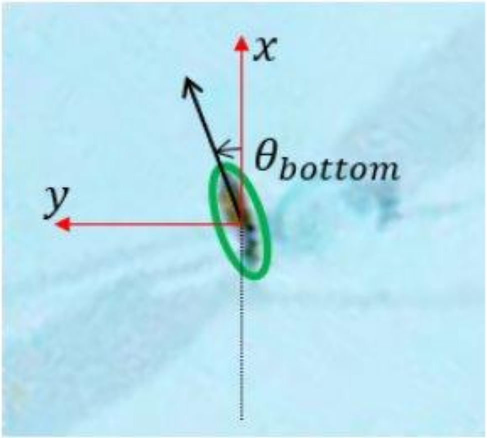

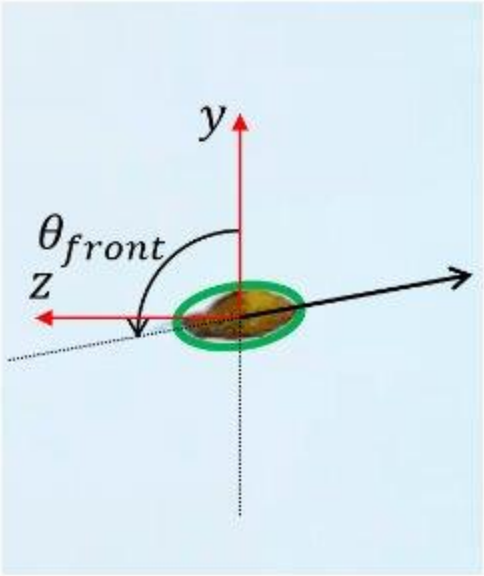

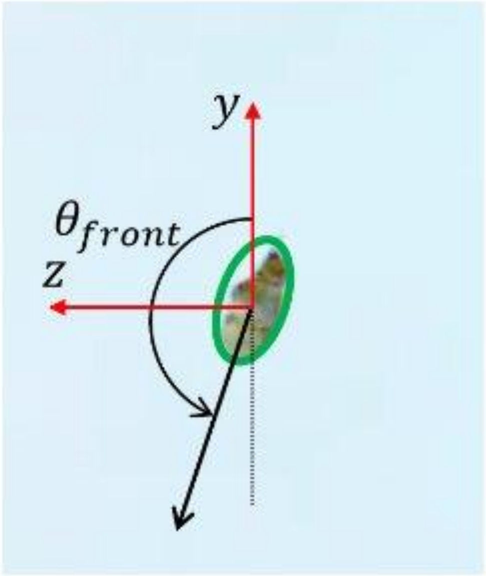

COMPUTING ALPHA AND BETA

- $\theta_{bottom} = \alpha$
- $\beta = \tan^{-1}(\tan(\theta_{front})\sin(\alpha))$
- $\boldsymbol{x_1}$ can be computed via a spherical coordinate transformation
  - $x = \cos(\beta)\cos(\alpha)$
  - $y = \cos(\beta)\sin(\alpha)$
  - $z = \sin(\beta)$

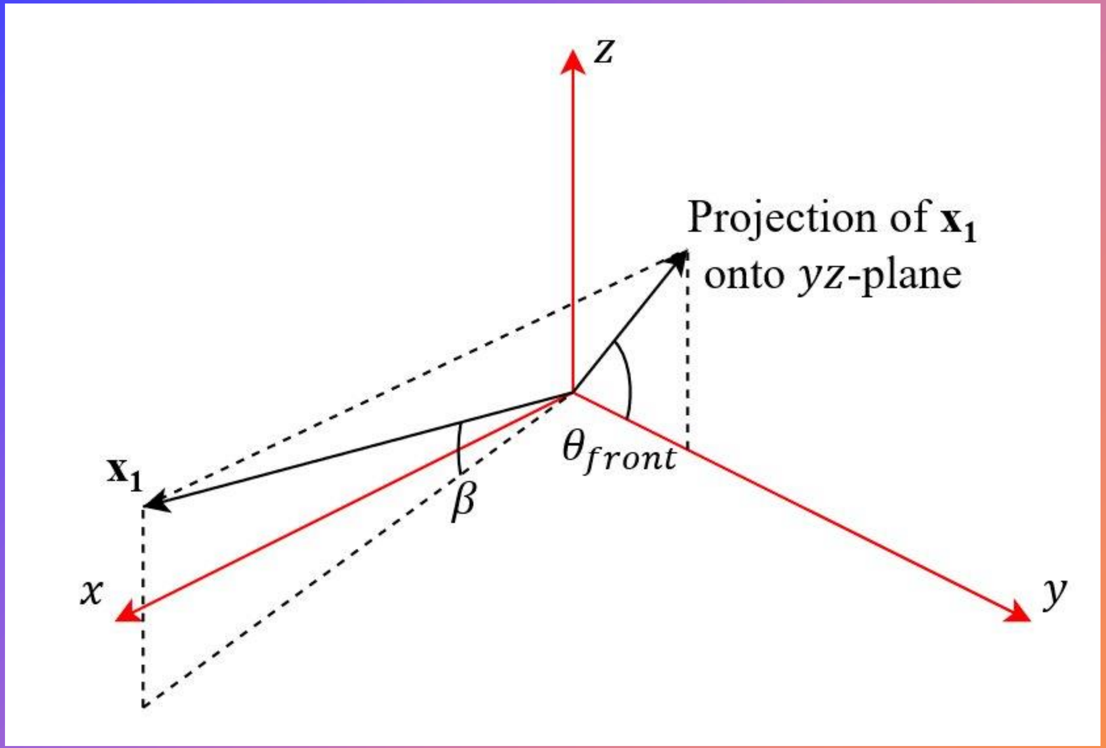

NORMAL VECTOR

- Eccentricity
  - Min: y = 0
  - Max: x = 0
- x_2 is normal to x_1
  - Body Axis
  - Useful for tracking properties (e.g. coning angle) during the transition phase

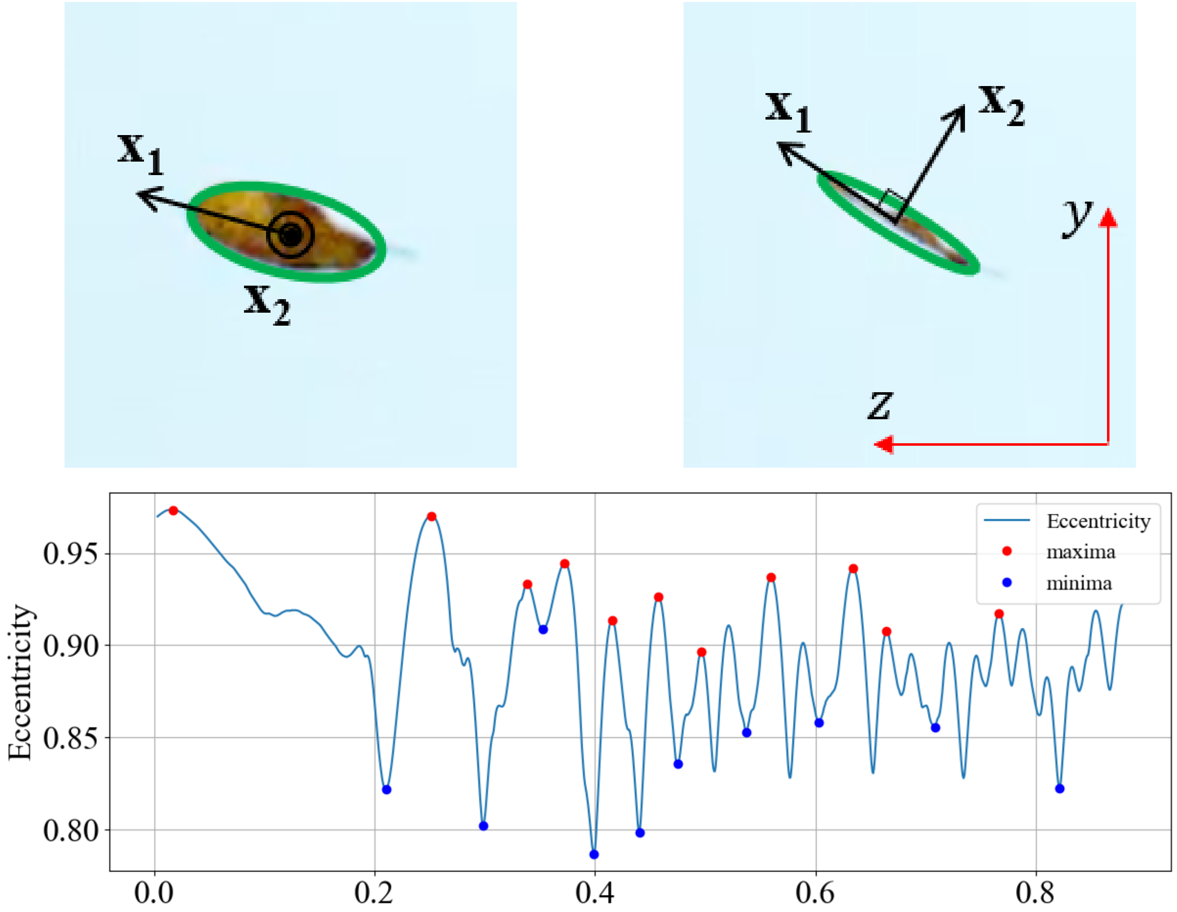

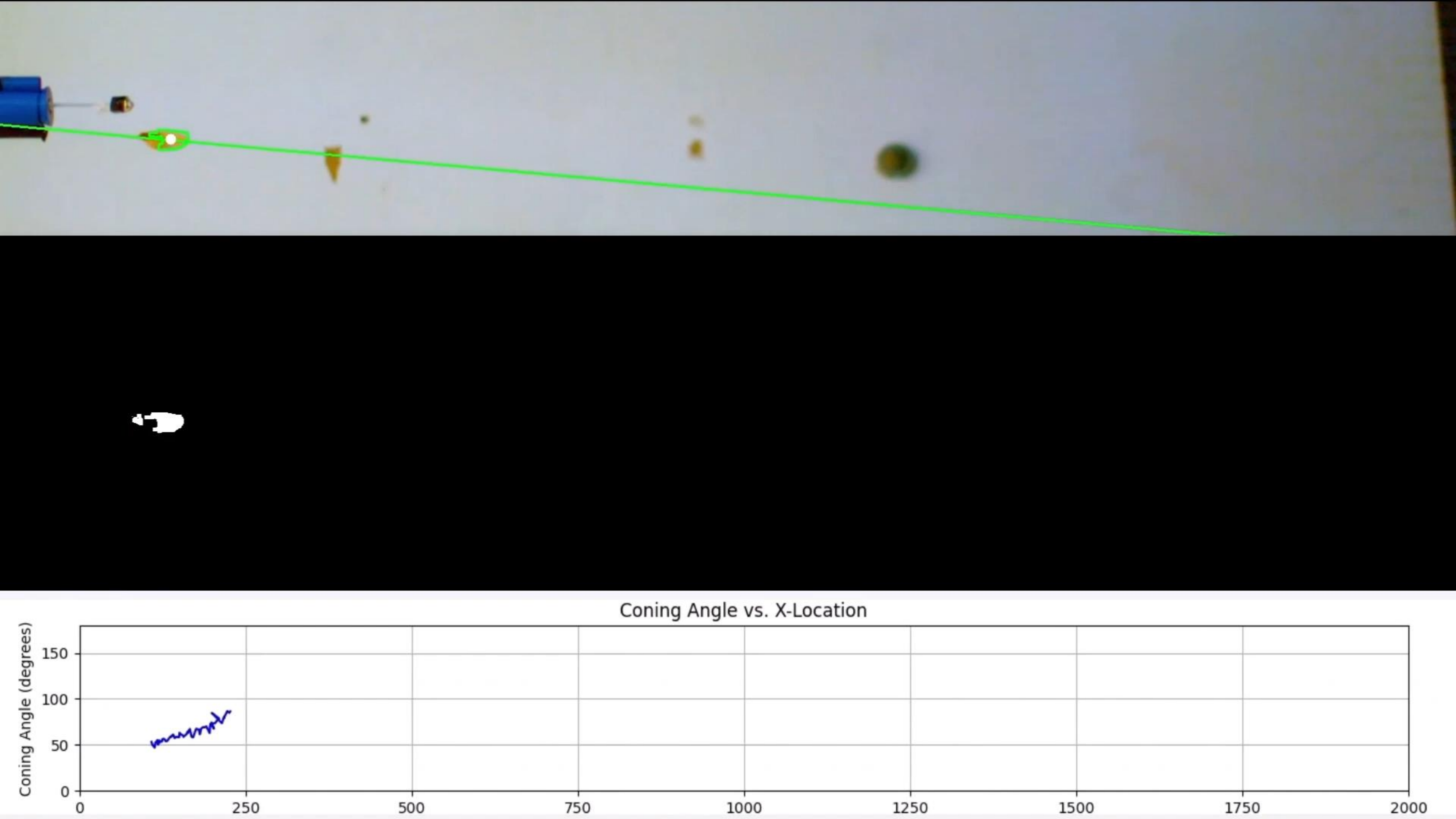
Coning Angle vs. X-Location
Coning Angle (degrees)
0
50
100
150
0
250
500
750
1000
1250
1500
1750
2000

SYMBOLS AND EQUATIONS

Variable	Symbol	Definition	Equation
Position	z	Position along the z axis	N/A
Velocity	v	Descent Speed	$v_z = \frac{\Delta z}{\Delta t} = \frac{z_{n+1} - z_n}{t_{n+1} - t_n}$
Acceleration	a	Descent Acceleration	$a_z = \frac{\Delta v_z}{\Delta t} = \frac{v_{n+1} - v_n}{t_{n+1} - t_n}$
Net Force	$F_{net\ z}$	Total Force experienced by the speed	$\sum ma_z = mg - F_z$
Thrust	T	Thrust generated by the seed	$F_{z\ steady\ state} = T = m * (g - a)$

Table 1

PRELIMINARY RESULTS

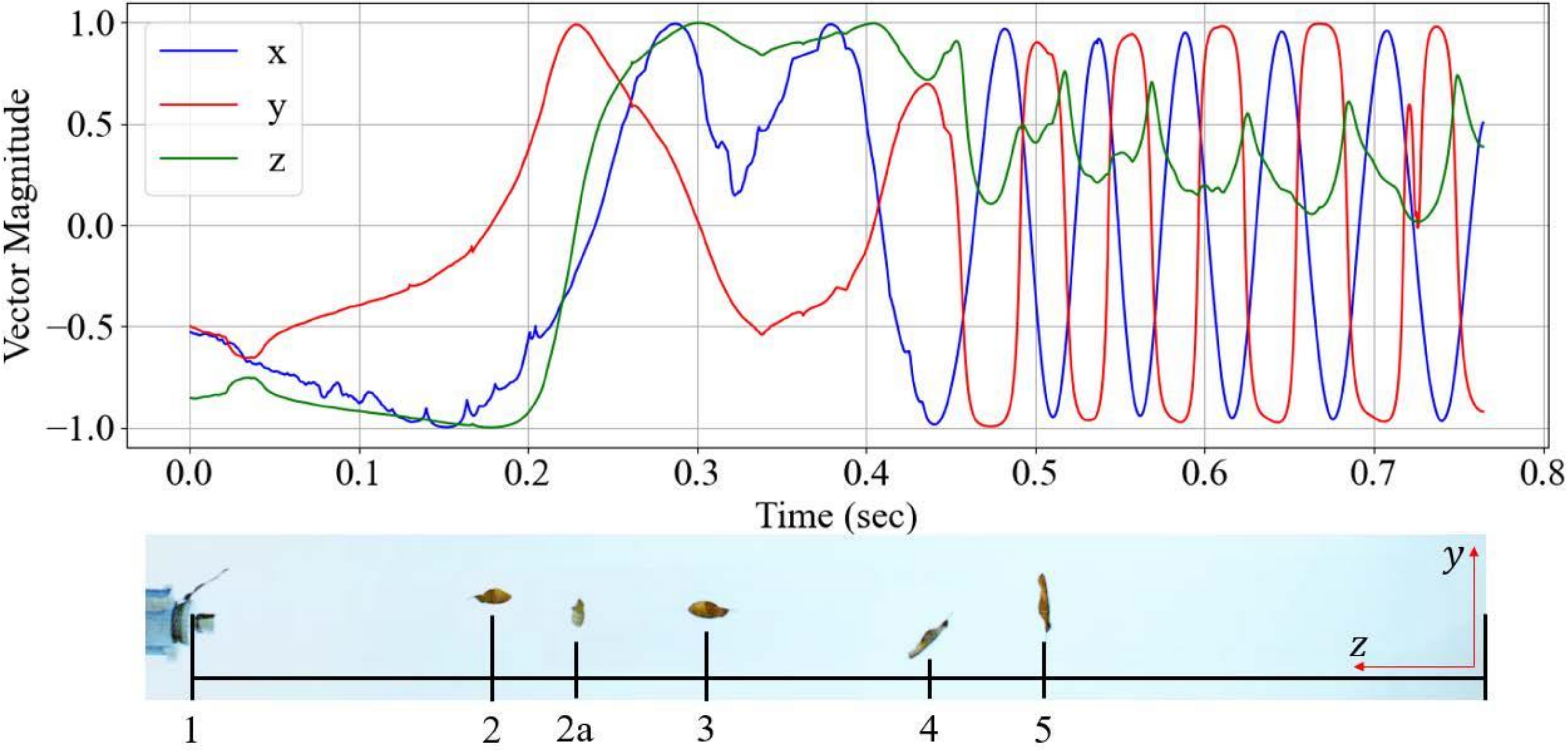

Vector Magnitude
Time (sec)
x
y
z
1.0
0.5
0.0
−0.5
−1.0
0.0
0.1
0.2
0.3
0.4
0.5
0.6
0.7
0.8
y
z
1
2
2a
3
4
5

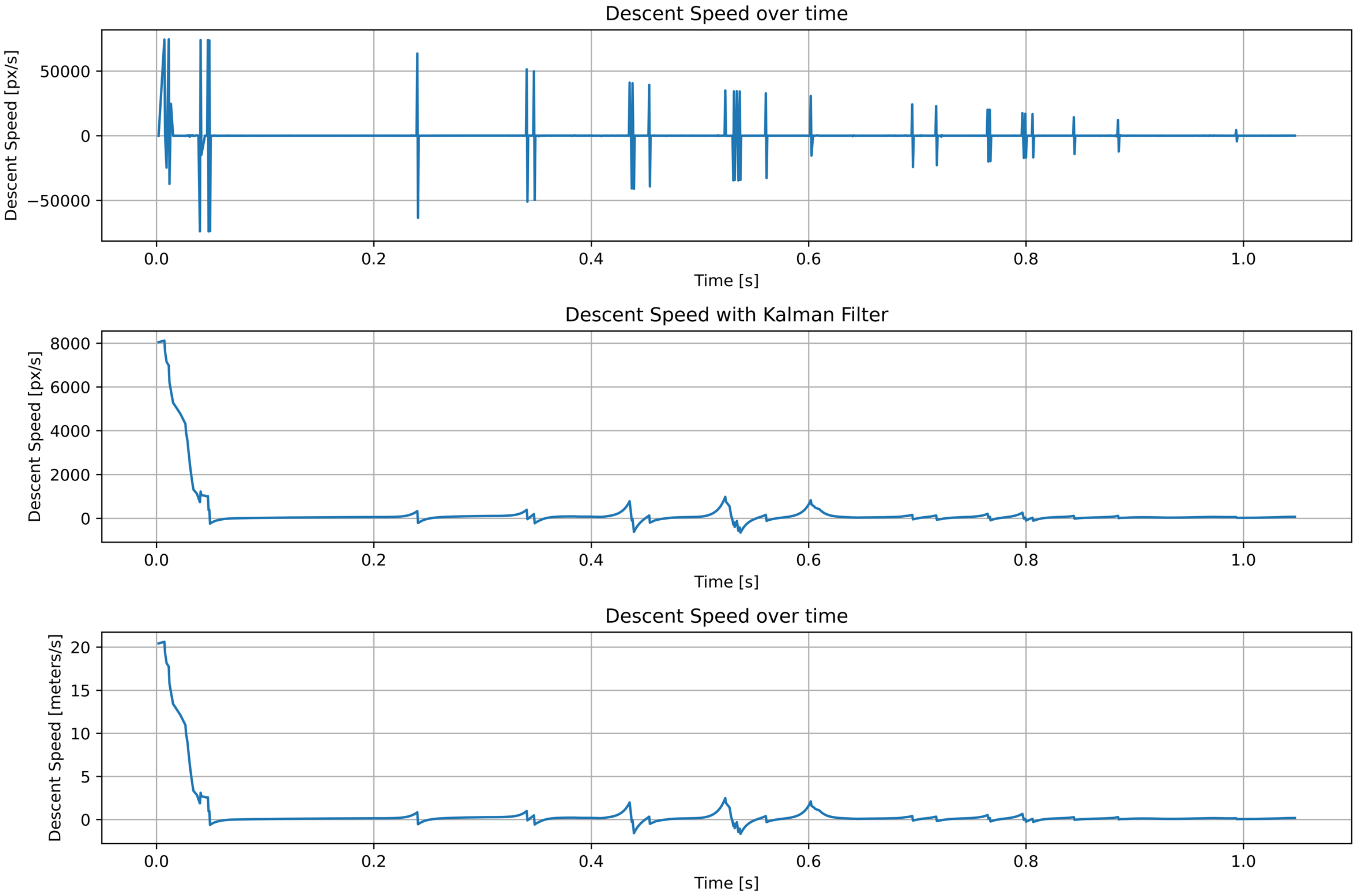

Descent Speed over time
Descent Speed [px/s]
50000
0
−50000
0.0
0.2
0.4
0.6
0.8
1.0
Time [s]
Descent Speed with Kalman Filter
Descent Speed [px/s]
8000
6000
4000
2000
0
0.0
0.2
0.4
0.6
0.8
1.0
Time [s]
Descent Speed over time
Descent Speed [meters/s]
20
15
10
5
0
0.0
0.2
0.4
0.6
0.8
1.0
Time [s]

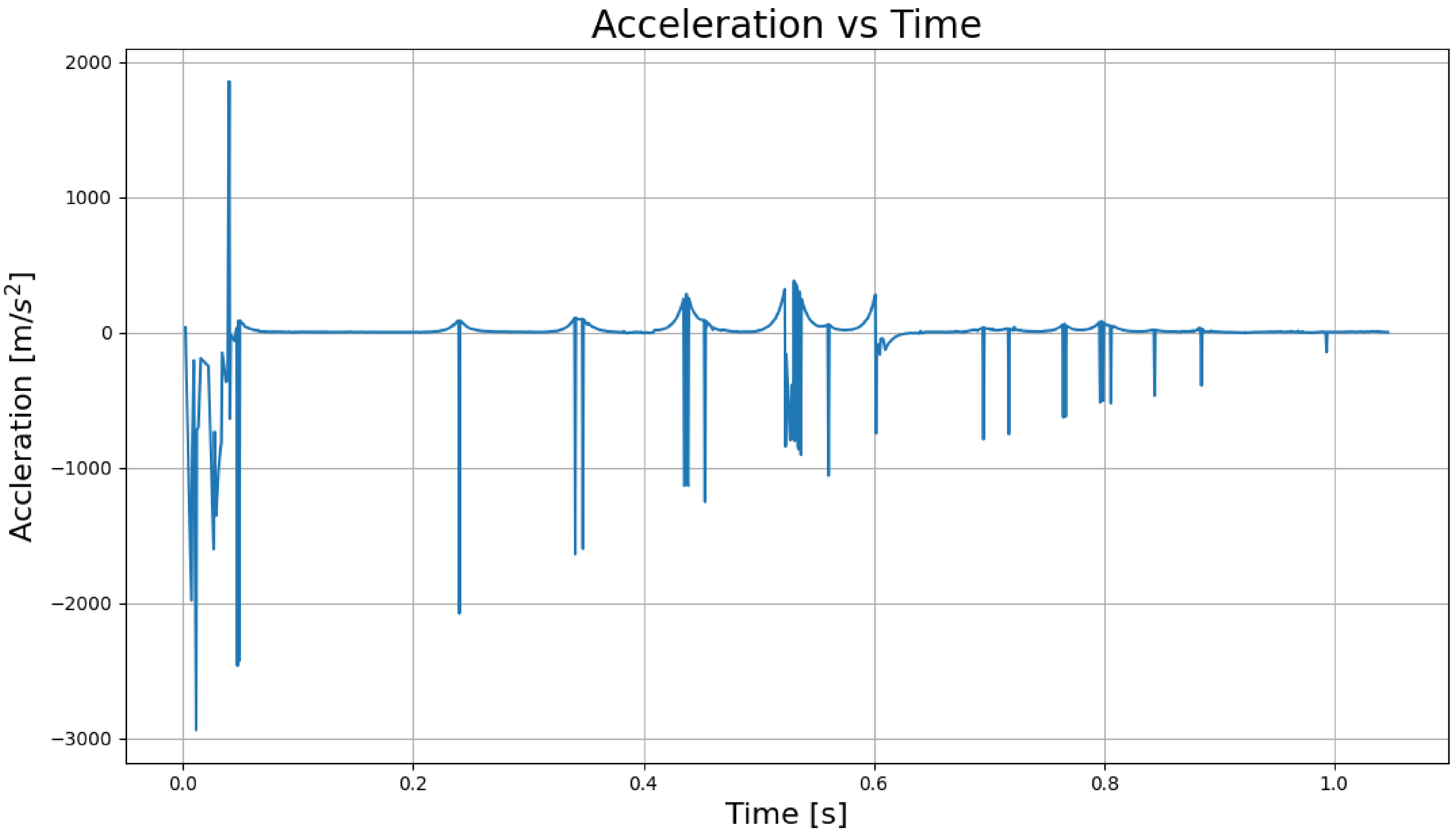

Acceleration vs Time
Accleration [m/s^2]
Time [s]
2000
1000
0
−1000
−2000
−3000
0.0
0.2
0.4
0.6
0.8
1.0

THRUST RESULTS

ID	Transition	Mass [g]	Aspect Ratio	RPM	Thrust [mN]	Specific Thrust [mN/g]
003	Fast	0.4	3.19	4750	2.96	7.38
007	Average	0.5	3.60	6680	3.89	7.79
047	Slow	0.6	3.71	3330	4.68	7.81

Table 2

CONCLUSION

SUMMARY

- Transition:
  - Region 1: The samara builds speed in free fall
  - Region 2: Drag causes the samara to flip, spin and flatten
  - Region 3: After 1 rotation, the descent speed slows completing transition
- Seed performance is consistent across multiple drops
- Non-monotonic trend with an average specific thrust ratio of 7.7 mN/g

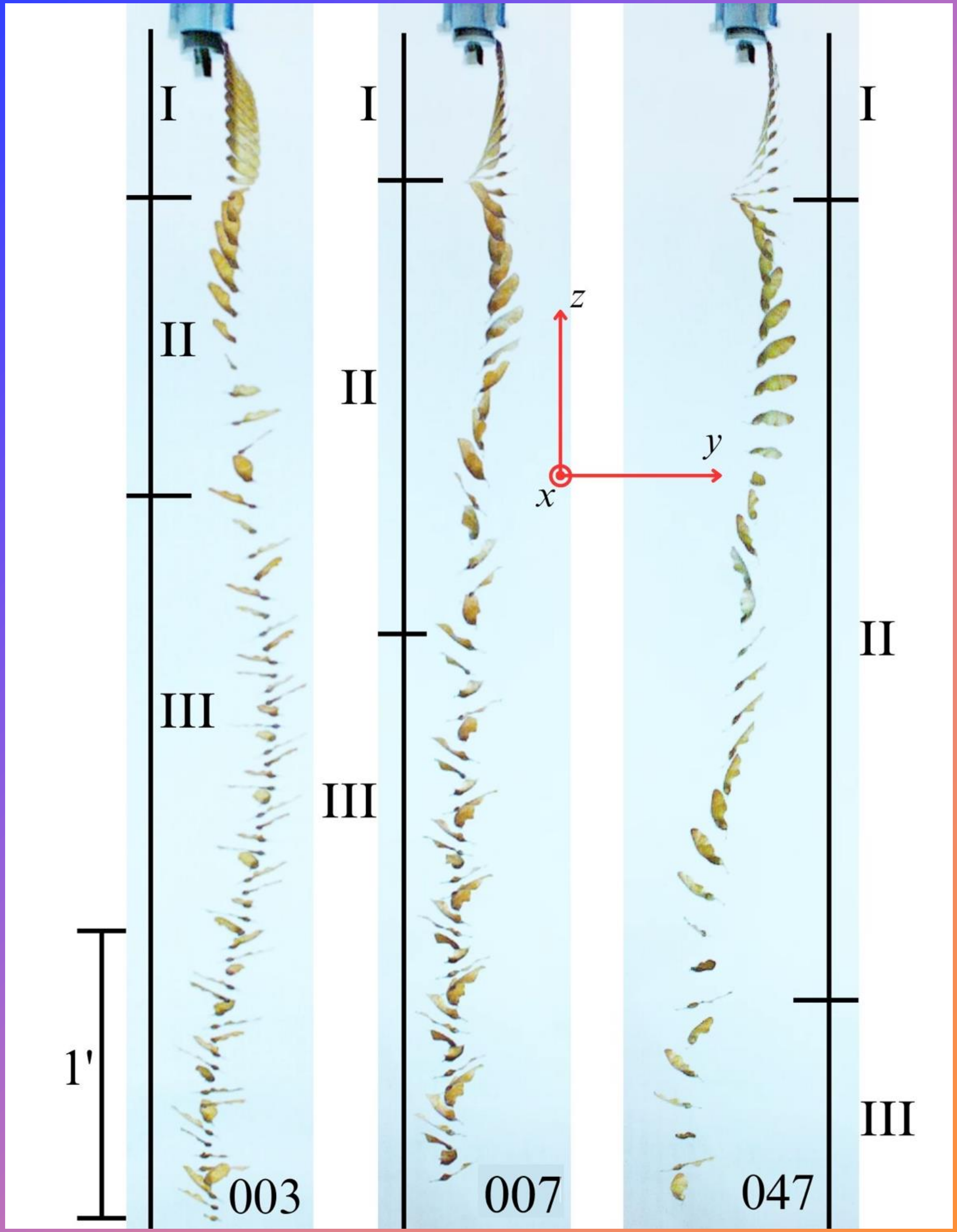

FAQ

Why use image recognition?

Why create Body Axis vectors x_1 and x_2?

Why not C_T?

$$T = \left(\frac{v_\infty^2}{4} + \frac{v_{tip}^2}{6}\right) * \rho * \mathrm{C_T} * \mathrm{A}$$

Why not C_Q?

$$Q = C_Q * \rho * \omega^2 * D^5$$

$$\Rightarrow C_{D_0} \leq 4\pi \left(\sqrt{1 + \left(\frac{v_{0,e}}{r\dot{\phi}_e}\right)^2} + \frac{\left(\frac{v_{0,e}}{r\dot{\phi}_e}\right)^2}{2\left(1 + \left(\frac{v_{0,e}}{r\dot{\phi}_e}\right)^2\right)} - 1 \right)$$

Resolution	Framerate	Exposure Time	Aperture	F-Stop
800x1280	1500 FPS	330 μs	4.0	1.2

CAMERA SPECS

- Phantom TMX 5010
- 1280px by 800px resolution
- Capable of 50,525 fps at full resolution
- Used 1500 FPS for testing
- Good balance of speed and exposure
- No motion blur
- Canon 50mm lens

DROPPER AND CAMERA

Figure 9, Reference 16

Figure 10, Reference 16

3D SCANS

Figure 6 Reference 16

Figure 7 Reference 16

GEOMETRIC PARAMETERS & CAMERA VIEW

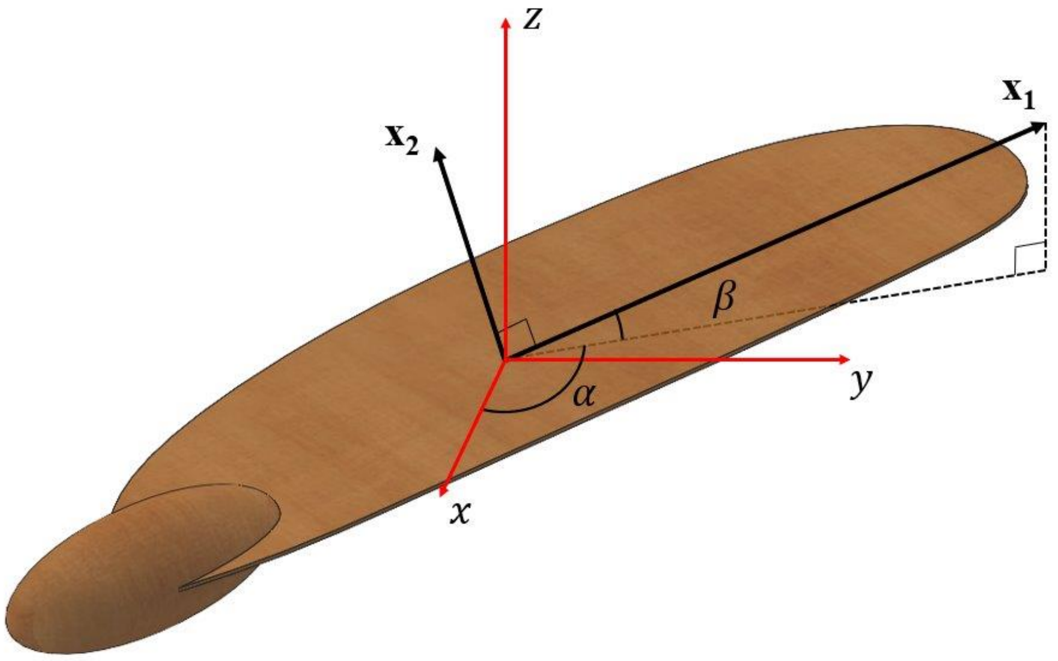

Figure 11, Reference 16

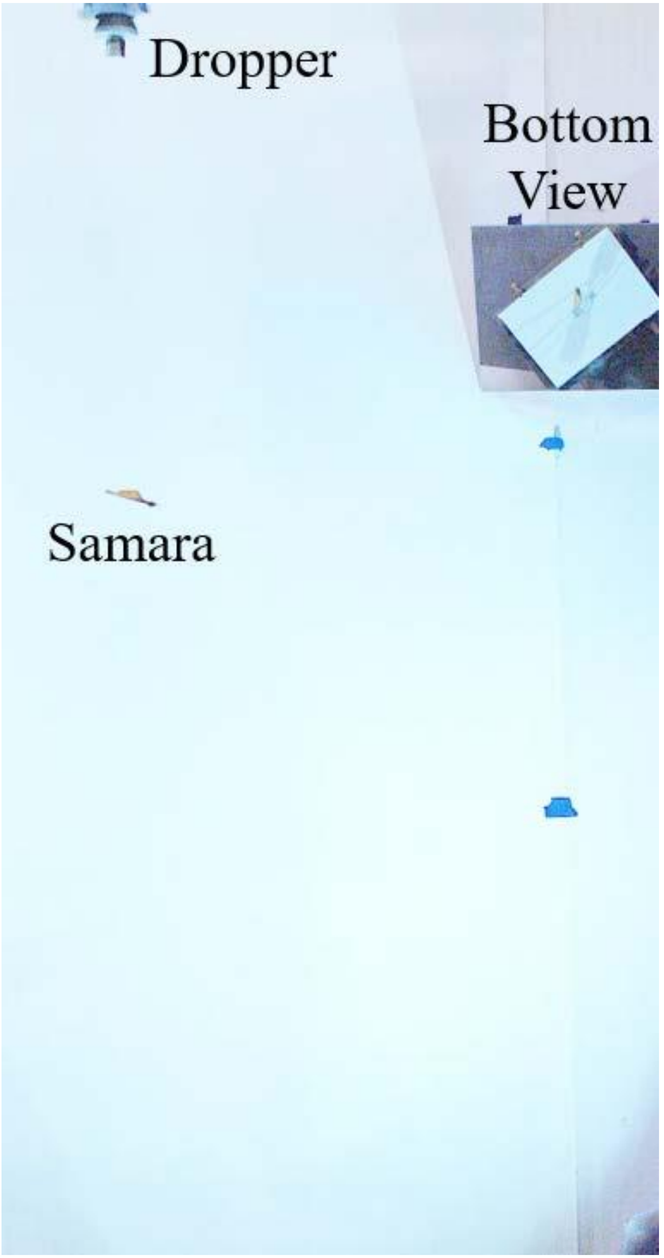

Figure 12, Reference 16